AN INVESTIGATION OF SPLITTER PLATES FOR SUPERSONIC TWIN INLETS

By John B. Peterson, Jr.

NASA Langley Research Center
Langley Station, Hampton, Va.

Presented at the Agard Specialist Meeting
on Aerodynamics of Power Plant Installation

Tullahoma, Tennessee
October 25-27, 1965

NATIONAL AERONAUTICS AND SPACE ADMINISTRATION
WASHINGTON

SUMMARY

34997

An experimental investigation was conducted to determine the ability of various splitter plates to isolate twin inlets aerodynamically such that in the event that one inlet is unstarted, the operation of the other inlet will not be affected. The effects of pylon height, inlet mass flow, and inlet yaw, on the performance of splitter plates were investigated. A pylon mounted external-internal compression inlet model was used and the tests were made at a Mach number of 2.5 and a Reynolds number based on cowl diameter of 10.8×10^6 (approximately full-scale flight conditions for an aircraft such as a supersonic transport). It was determined that splitter plates of a practical size will isolate an unstarted inlet at least as long as the mass-flow ratio is maintained above approximately 0.65.

Author

NOTATION

A_i	inlet capture area, $\frac{1}{2}\frac{\pi D^2}{4}$, 9.82 in^2 (63.35 cm^2)
A_t	inlet throat area, 5.10 in^2 (32.9 cm^2)
D	cowl diameter, 5 in. (12.7 cm)
$\dot{m}_1$	mass-flow rate through stream tube of area A_i at conditions behind splitter-plate shock
$\dot{m}_2$	measured inlet mass-flow rate
p_t	total pressure
R	Reynolds number
ψ	angle of yaw, degrees

Subscripts:

2	conditions at the diffuser exit
∞	conditions in free stream
δ	based on boundary-layer total thickness

AN INVESTIGATION OF SPLITTER PLATES FOR SUPERSONIC TWIN INLETS

By John B. Peterson, Jr.*

1. INTRODUCTION

The location and design of the propulsion system is important to the performance and safety of an aircraft such as a supersonic transport. A number of investigations (ref. 1 and other proprietary investigations) have been conducted to determine the effects of various arrangements of the propulsion packages relative to one another. Problems arise from the fact that unstarts of mixed compression inlets cannot presently be completely eliminated, and that the unstart of one inlet must not initiate the unstart of an adjacent one, since the two unstarted adjacent inlets would precipitate extreme rolling and yawing moments.

One type of engine pod which has been proposed is the twin inlet design (ref. 2). Examples of this arrangement are shown in figures 1 and 2. This arrangement places two propulsion packages in a single nacelle and attempts to insure independent operation by employing a splitter plate which divides the nacelle and extends forward, isolating the two inlets.

There are a number of advantages to this twin-inlet configuration. First, the total wetted area of all the nacelles is reduced with corresponding reductions in skin-friction drag. Secondly, important benefits are obtained from the splitter plate which is used as a compression surface to decrease inlet size, increase inlet pressure recovery, and reduce flow distortions caused by yaw. In addition, this arrangement allows placement of the engines more nearly on the centerline of the aircraft which is

---

*Aerospace Engineer, NASA Langley Research Center, Langley Station, Hampton, Va.

desirable for structural and aerodynamic reasons (for example, reduction in the asymmetric thrust and reduction in roll moment of inertia).

These considerations make the twin-inlet arrangement a highly favorable design. However, the feasibility of the design hinges upon the ability of the splitter plate to isolate the two inlets aerodynamically such that in the case of an unstart of one inlet, the other inlet would be unaffected. This splitter plate must be of a practical size such that the drag and weight do not override the advantages of the arrangement.

An investigation was conducted in the NASA Langley 20-inch variable supersonic tunnel to determine the ability of splitter plates of practical size to isolate aerodynamically an unstarted twin-inlet model. The investigation was carried out at a Mach number of 2.5 and a Reynolds number based on cowl diameter of 10.8×10^6, which are very near full-scale flight conditions under the wing of proposed supersonic transports flying at 65,000 feet (19,812 meters) with a 6.5-foot (1.98 meter) cowl diameter. The effects of pylon height, yaw, and inlet mass flow on splitter-plate performance were investigated.

2. APPARATUS

2.1. Model

The basic model consisted of a semicircular inlet which simulated one-half of a twin-inlet configuration which was pylon mounted to a plate simulating the wing. Photographs and drawings of the model are presented in figures 3 and 4. The inlet was mounted upside down from the actual flight configuration for convenience in handling. The plate simulating the wing was parallel to the free stream; thus, the model has no wing compression. Pressure probes were used in place of a second twin inlet and will be discussed later.

The center body of the semicircular external-internal compression inlet was fixed at the design Mach number position and the internal contraction prohibited the inlet from starting throughout the investigation. While this did not allow examination of the effects of the initial unstart pulse which results when an external-internal compression inlet unstarts, the magnitude of this initial pulse is only slightly greater than the pulses of the unstarted inlet flow field which follows (unpublished industry data and ref. 1). Some detail tailoring of the successful splitter plates, however, may be necessary to isolate the first unstart shock.

The half-cone center body has a 12.5° half-angle; the inlet internal and external cowl lip angles at 0° and 5°, respectively; and the inlet contraction ratio A_t/A_i is 0.52. All splitter plates provided 2.5° of compression which reduced the local Mach number to 2.4 and the center body shock was directed toward the cowl lip at this design Mach number. Three pylon heights were investigated. The pylons positioned the cowl lip 0.5, 0.25, and 0.10 of the inlet diameter D above the wing plate and were designated high, medium, and low pylons, respectively. Photographs, composite sketches, and dimensional drawings of the various splitter plates investigated are shown in figures 5, 6, and 7.

The fixed-wing plate was used to simulate the undersurface of the wing. It was necessary to simulate the wing because the shocks from the unstarted inlet might interact with the wing boundary layer and thereby allow disturbances to reach the opposite inlet. Since the interaction length is dependent upon Reynolds number based on boundary-layer thickness R_{δ} (ref. 3), it was decided to obtain the proper boundary-layer thickness by the use of distributed roughness on the wing plate. Number 120 carborundum was distributed over the first 15 inches (38.1 cm).

This allowed 4 to 5 inches (approximately 10 to 13 cm) on the surface of the plate, after the distributed roughness region, for the boundary layer to recover its normal shape before encountering any shocks.

2.2. Instrumentation

Pitot tubes were used in place of a second inlet to indicate if disturbances reached the other side of the splitter plate. This was done to reduce the complexity of the model. Also, since the tunnel-blockage area was reduced by elimination of the second inlet, a larger model could be used and full-scale Reynolds numbers were obtainable. The three pitot tubes were located at positions which would correspond to the two points where the cowl lip of a second twin inlet would join the splitter and at the midpoint between these two. A record of the pitot pressures was taken continuously during each run on a direct readout oscillograph.

2.3. Flow Visualization

In order to aid in the evaluation of the effectiveness of the splitter plates, both schlieren and shadowgraph movies were obtained. The schlierens picture all the flow except that which was blocked from view by the splitter plates.

A unique shadowgraph method was used to obtain movies of the flow field on the splitter plates. (See fig. 8.) This method consisted of reflecting parallel light off the splitter plates, passing the reflected light through an achromatic convex lens, and focusing the light into a 16-mm Fastex camera operating at 2000 frames per second. Flow separations and shocks on the splitter plates may be seen clearly on the shadowgraphs since light rays are deflected by these disturbances. The edges of the shadowgraphs were of poor quality because the splitter-plate edges were rounded slightly in the polishing process.

2.4. Tests

Tests were conducted with an open-diffuser exit and with reduced mass flow. In both cases, the mass flow was measured by nozzles in the diffuser exit. With the diffuser exit open, a complete series of tests was conducted at various pylon heights and angles of yaw. Open-exit condition tests were considered the most significant for the following reasons. There are numerous causes of inlet unstarts and the mass flow through an unstarted inlet normally depends on exactly what type of unstart has occurred. However, future supersonic inlets should incorporate subsonic bypass doors which, although possibly unable to completely eliminate inlet unstarts, will react very rapidly. These bypass doors will pass any excess mass flow entering the unstarted inlet which cannot pass through the engine, as may be the case in certain types of unstarts. Thus, the unstarted inlet mass-flow ratio will depend only on how much internal contraction the inlet has and the results with the diffuser exit open may be considered to accurately simulate actual unstart conditions. A limited number of reduced mass-flow tests were conducted which serve to indicate the performance of the splitter plates in the event that the subsonic bypass doors fail to open or do not react rapidly enough to prevent reduced mass flows in the unstarted inlet.

3. DISCUSSION

3.1. Inlet Flow Field for the Open-Diffuser Exit Case

A schematic drawing of the unstarted inlet flow field is shown in figure 9, which is representative of the flow field on the splitter plate, regardless of the shape of the splitter plate, pylon height, or angle of yaw. The flow field of the unstarted inlet was steady, indicating that this particular inlet had some degree of subcritical stability. This basic inlet flow field consisted of a cone separation with the accompanying separation shock followed by a normal shock in front of the inlet cowl. There are also two "ridge" lines. The ridge line, where the plate boundary-layer flow has been deflected outward away from the cone, is a phenomena of the glancing interaction of a shock wave with a turbulent boundary layer and is caused by upstream pressure influences of the separation shock. See references 4 and 5 for a discussion of ridge lines. Figure 10 is a composite photograph made up of a schlieren showing all the flow except that blocked from view by the splitter plate and a shadowgraph picturing the flow on the splitter plate. For clarity, the outline of the model has been marked. This photograph shows a typical flow field about the complete model and various disturbances are pointed out in the figure. The shocks reflected from the tunnel floor were shocks from supporting struts and the wing leading edge. None of these shocks affected the pitot pressures at any time.

3.2. Splitter-Plate Effectiveness for the Open-Diffuser Exit Case

Results with the high pylon are presented first. Figures 10 and 11(a), (b), and (c) show the inlet flow fields for splitter plates 1, 2, 3, and 4, respectively, and the corresponding pressure traces are presented in figure 12(a), (b), (c), and (d). Considering splitter plates 1, 2, and 3 first, it is seen that the flow fields are all very similar and that the pressure traces for these plates are all steady. Thus, all three plates are effective in isolating the unstarted inlet at the high pylon height even though plates 2 and 3 are somewhat smaller than splitter plate 1. These tests indicate that it is not necessary for a successful splitter plate to extend beyond the tip of the conical center body.

When splitter plate 4 was used with the high pylon, the results shown in figure 12(d) indicate that the inlet flow field was not isolated.

Although the flow field of the unstarted inlet (fig. 11(c)) appears the same as in the previous photographs for plates 1, 2, and 3, the upper and lower pitot pressure probes were being disturbed. The pressure relieving effects at the edges of the splitter plates tend to allow disturbances to flow around the edges of the plate and evidently the disturbances negotiated the turn on splitter plate 4 and reached the pitot pressure probes because the upper and lower edges of plate 4 did not extend past the cowl lip. It is apparent that some extension is necessary and it has already been shown that splitter plate 3 with its 7.5-percent inlet-cowl diameter extensions is successful in preventing the unstarted flow field from spilling around the upper and lower edges. The results for splitter plates 1, 2, and 3 at the medium pylon height of 0.25D were the same as at the high pylon heights.

The three plates were next tested at the low pylon height of 0.1D. In this case, splitter plates 1 and 2 were again successful in isolating the unstarted inlet flow field. It is significant that both of these plates have lower edges which lie on the surface of the wing. Splitter plate 3, however, leaves a gap of 0.125 inch (0.32 cm) between the lower edge of the splitter plate and the surface of the wing plate at the low pylon height. A composite schlieren photograph of the flow on splitter plate 3 is shown in figure 13 and the accompanying pitot pressure traces are shown in figure 14. The pressure disturbances shown on the lower pressure probe in figure 14 indicate that splitter plate 3 was ineffective at this pylon height. Evidently the flow field wing boundary-layer interaction propagated through the gap to disturb the lower probe, thus, in order to isolate twin inlets at low pylon heights, it is necessary to have the splitter plate and wing connect. In an actual practical configuration such an arrangement would be desirable also for structural reasons.

Splitter plates 1, 2, and 3 were also tested at all three pylon heights at an angle of yaw of 6° with the unstarted inlet windward. Although adverse effects might have been expected, in no case was the ability of the splitter plates to isolate the unstarted inlet altered by 6° of yaw.

3.3. Splitter-Plate Effectiveness for the Reduced Mass-Flow Case

A limited number of tests were conducted in which the mass-flow ratio was reduced below 0.72 (open-exit condition). Photographs of the general sequence of events when splitter plate 1 was tested at reduced mass flows is shown in figures 15 and 16. The numbers on the figures correspond to frame numbers of the movies. As the mass flow was reduced below 0.72, buzz of high frequency began at a value of $\dot{m}_2/\dot{m}_1$ of about 0.65. With further mass-flow reduction, the buzz changed to a lower frequency oscillation of larger amplitude and the high frequency mode was superimposed on this oscillation. The buzz became more severe as the mass flow was reduced still further. When plate 1 first failed (i.e., became ineffective) at $\frac{\dot{m}_2}{\dot{m}_1} = 0.57$, the upper and lower pitot pressures were disturbed. With lower mass flows, the probe disturbances were more severe and at zero mass flow all three probes were disturbed. The inlet buzz was so strong at zero mass flow that even the largest splitter plate, number 5, was unable to isolate any of the probes from disturbances.

It was found that this general sequence of events occurred with reduced mass flow for splitter plates 1 and 3 at all pylon heights and for angles of yaw of 0° and 6°. (Plate 2 results are discussed later.) Figure 17(a) presents the performance of splitter plates 1 and 3 for various mass flows and $\psi = 0^\circ$. Points where the splitter plates were ineffective are denoted by flagged symbols. From this figure it is seen that plates 1 and 3 are successful in isolating the unstarted inlet down to a mass-flow ratio of about 0.65 but fail when the ratio is reduced to about 0.57. Plate 3 is, of course, never successful at the low pylon height because of the gap between the splitter plate and the wing surface.

The performance and inlet flow-field characteristics of splitter plate 2 at $\psi = 0^{\circ}$ shown in figure 17(b) were the same as for splitter plate 1 down to a mass-flow ratio of 0.64. As the mass flow was further reduced to 0.57 (the mass-flow ratio at which splitter plate 1 failed) plate 2 became ineffective at the medium pylon height where the lower pitot tube was disturbed but was still effective at the high and low pylon heights. When an attempt was made to reduce the mass flow further, the flow completely changed character to a steady separated condition and the mass flow dropped to 0.27. This condition is shown by the shadowgraphs in figure 17(b). Since separation occurred at one of the corners on the front of the plate, it appears that the separation may have been induced by slight pressure gradients caused by the conical flow field that the corners generate. The question of whether plate 2 was successful between a mass-flow ratio of 0.57 and 0.27 cannot be determined because mass flows in this range were unobtainable, but at best, any success was marginal inasmuch as ineffectiveness of the plate was already indicated for the medium pylon height at a mass-flow ratio of 0.57.

Some reduced mass-flow tests were also conducted at $\phi = 6^{\circ}$ and results are shown in figure 18. Plates 1 and 2 were successful down to a mass-flow ratio of about 0.55, but plate 3 was only successful for the open-exit condition at a mass-flow ratio of 0.62. Plate 3 probably fails somewhat earlier than plates 1 and 2 because its upper and lower edges extend only 7.5-percent cowl diameters as compared to 10-percent cowl diameters for plates 1 and 2.

The most important conclusion to be drawn from the test with reduced mass flow is that reasonably sized splitter plates will continue to isolate an unstarted inlet at least down to a mass-flow ratio of approximately 0.65.

4. CONCLUSIONS

An investigation was made at a Mach number of 2.5 and a Reynolds number based on cowl diameter of 10.8×10^6 (approximately full-scale flight conditions for a supersonic transport) to determine the ability of various splitter plates to isolate an unstarted twin inlet. The investigation led to the following conclusions:

1. Splitter plates of practical size can isolate the unstarted twin inlet as long as the mass-flow ratio is maintained above approximately 0.65.

2. It is necessary for the upper and lower edges of successful splitter plates to extend above and below the cowl lip. (An extension of 7.5 percent of the cowl diameter was successful.) It is not necessary, however, for the splitter plate to extend beyond the tip of the conical center body.

3. Splitter plates of practical size are successful for yaw up to 6° with the unstarted inlet windward.

4. Pylon height has little effect except at very low heights where it is necessary that there be no gap between the splitter plate and the wing.

REFERENCES

1. Motycka, D. L.; and Murphy, J. B.: Inlet-to-Inlet Shock Interference Tests. Pratt and Whitney Aircraft Report PWA-2525, December 31, 1964. (NASA Contract NASZ-2079)
2. Robins, A. Warner; and Whitcomb, Richard T.: Additional Configurations Approaches. Preceedings of NASA Conference on Supersonic-Transport Feasibility Studies and Supporting Research. NASA TM X-905, 1963.
3. Hammitt, Dr. Andrew G.: Scale Effects in Turbulent Shock Wave Boundary-Layer Interactions. Proceedings of the Sixth Annual Conference on Fluid Mechanics, Held at University of Texas, Austin, Texas, September 1959.
4. Landrum, Emma Jean: A Study of a Mach Number of 2.01 of the Shock Boundary-Layer Interaction Resulting From the Deflection of a Wedge Mounted on a Bypass Plate. M. A. Thesis, The College of William and Mary in Virginia, June 1961.
5. Stanbrook, A.: An Experimental Study of the Glancing Interaction Between a Shock Wave and a Turbulent Boundary Layer. TN No. AERO 2701, Royal Aircraft Establishment, July 1960.

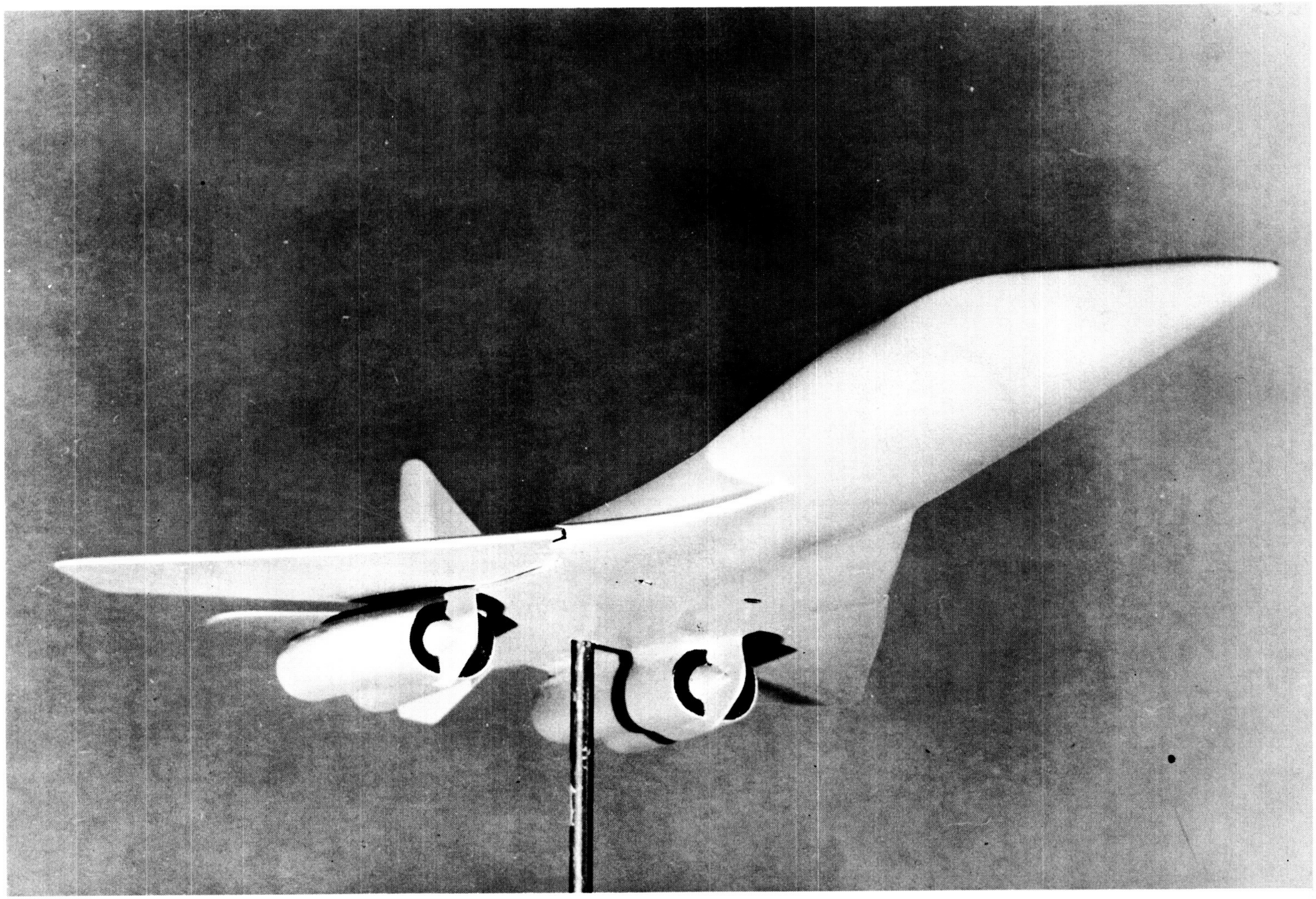

Figure 1.- Supersonic transport model with a twin-inlet propulsion system.

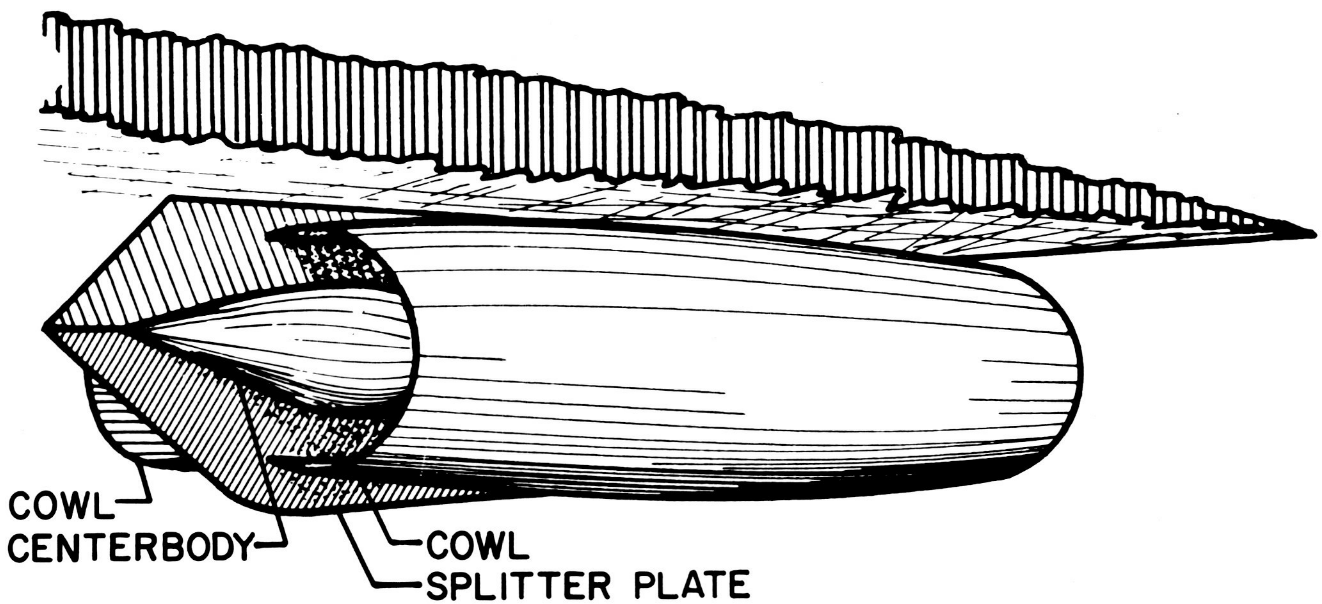

Figure 2.- Twin-inlet configuration.

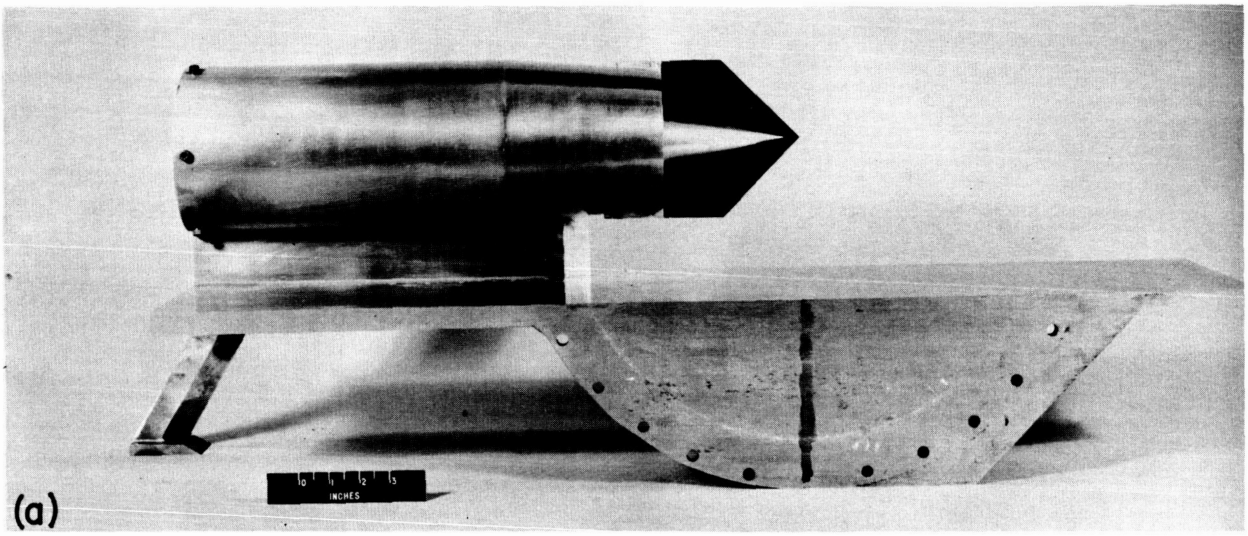

(a) Right side view.

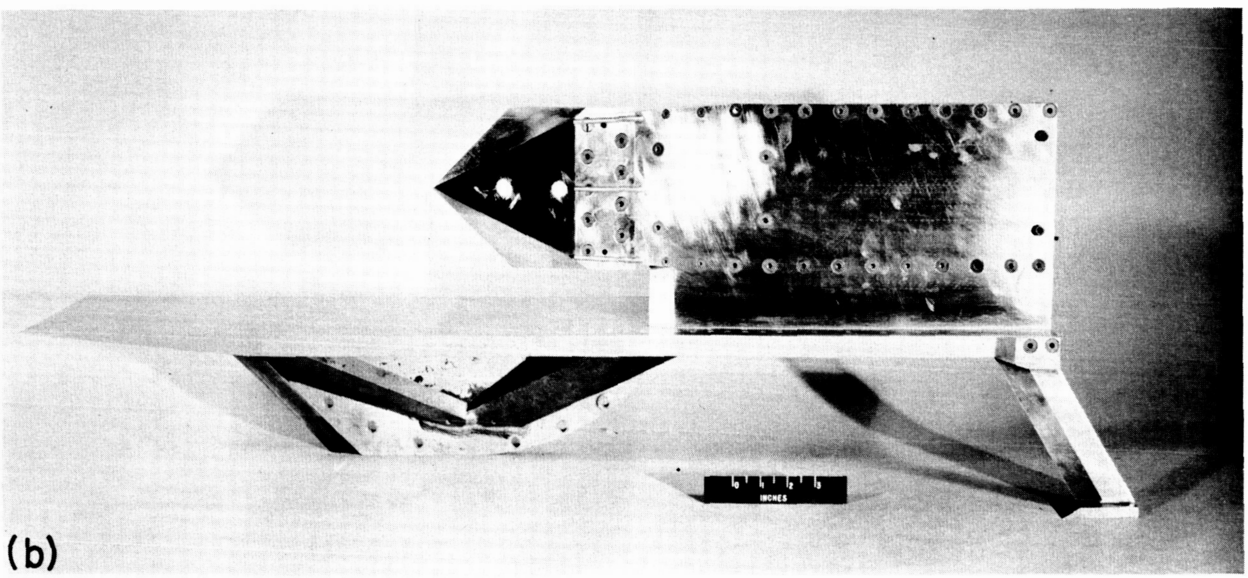

(b) Left side view.

Figure 3.- Wind-tunnel model.

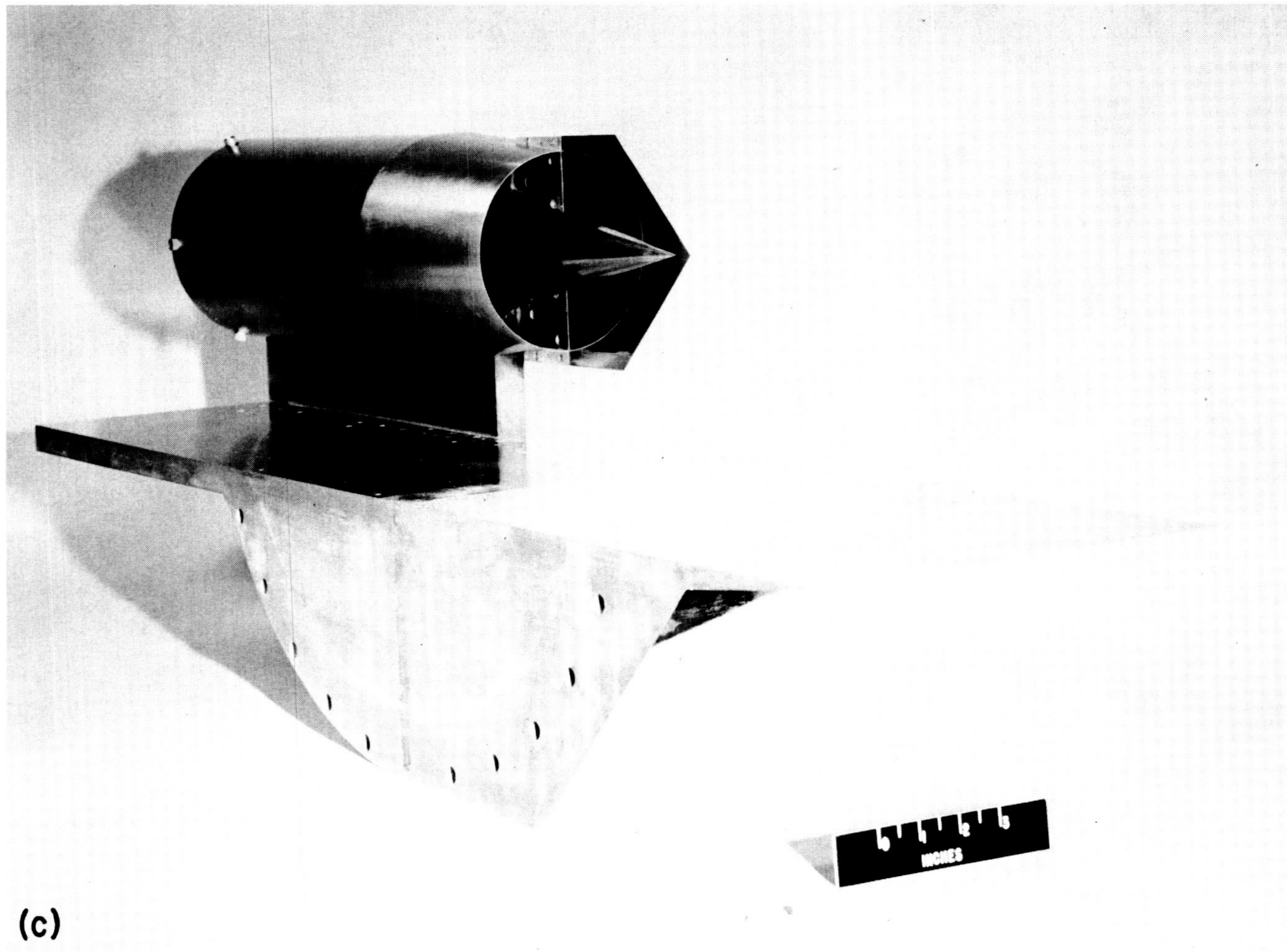

(c) Oblique view.

Figure 3.- Concluded.

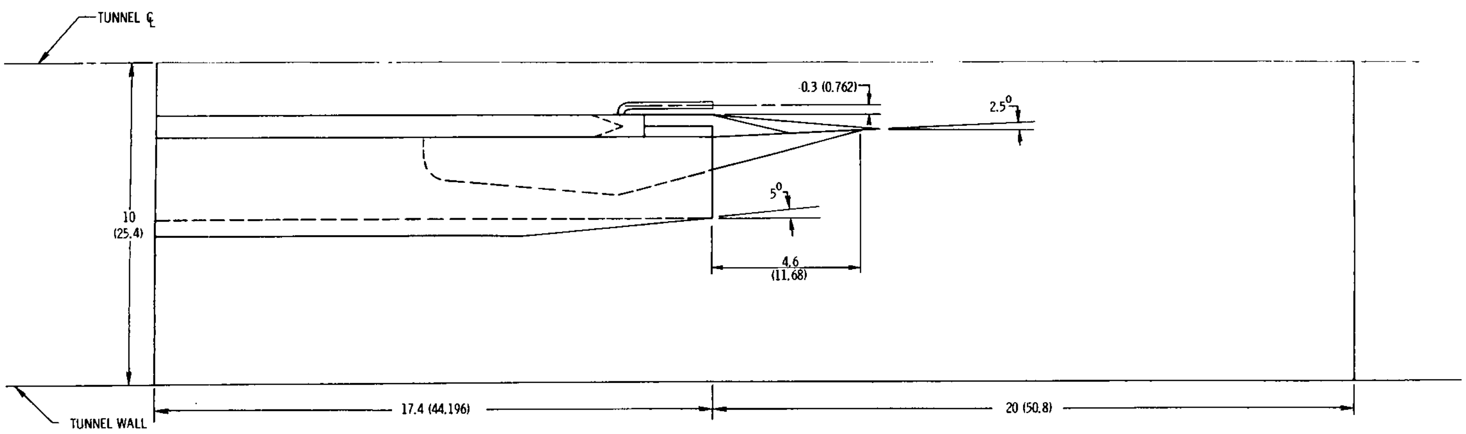

(a) Top view.

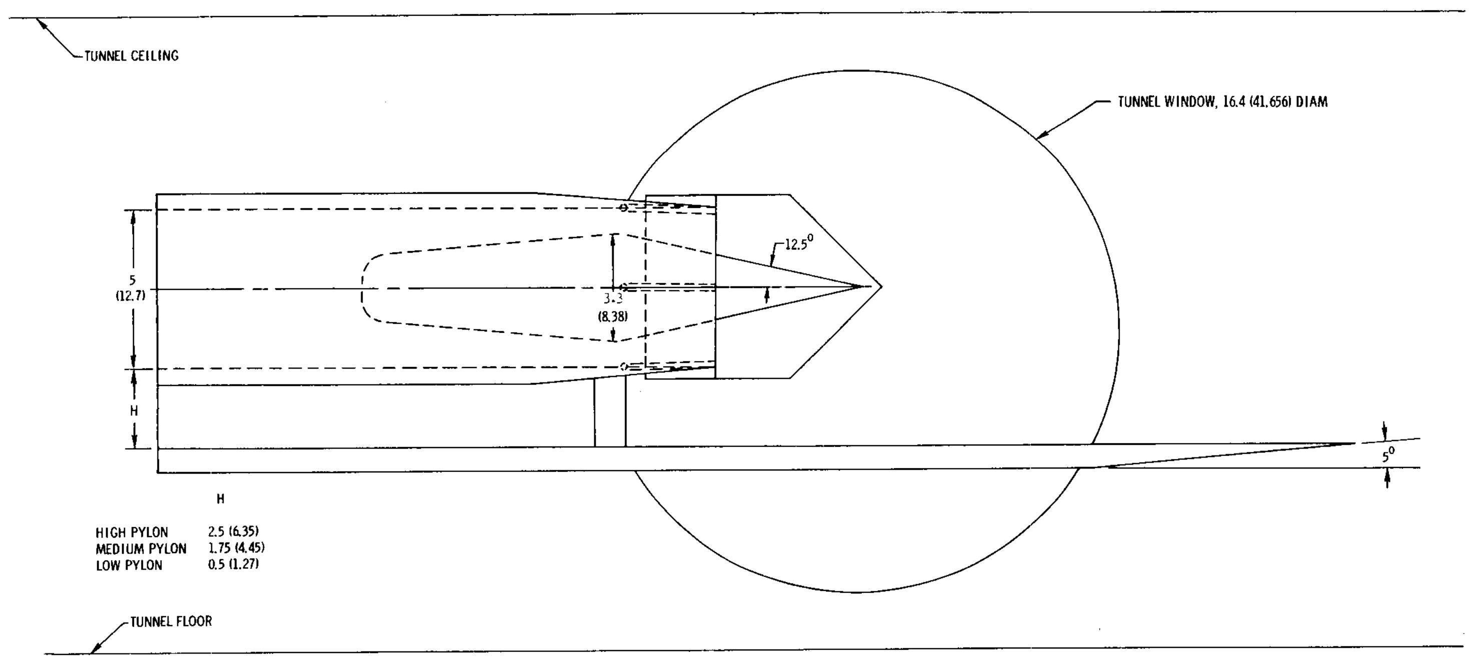

(b) Right side view.

Figure 4.- Drawings of wind-tunnel model. All dimensions in inches (dimensions in parenthesis in centimeters).

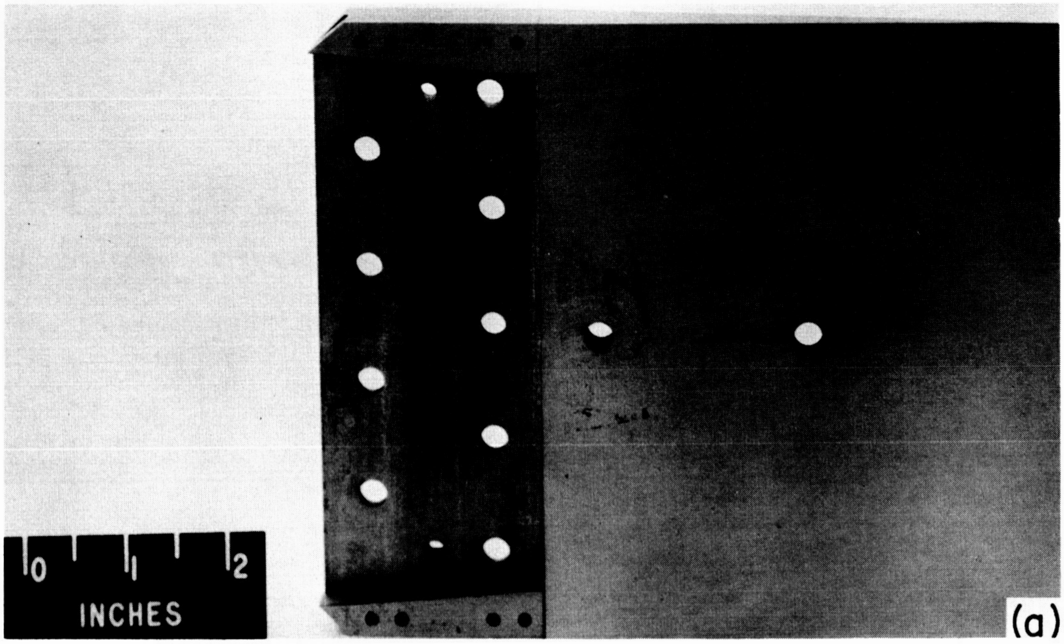

(a) Splitter plate 1.

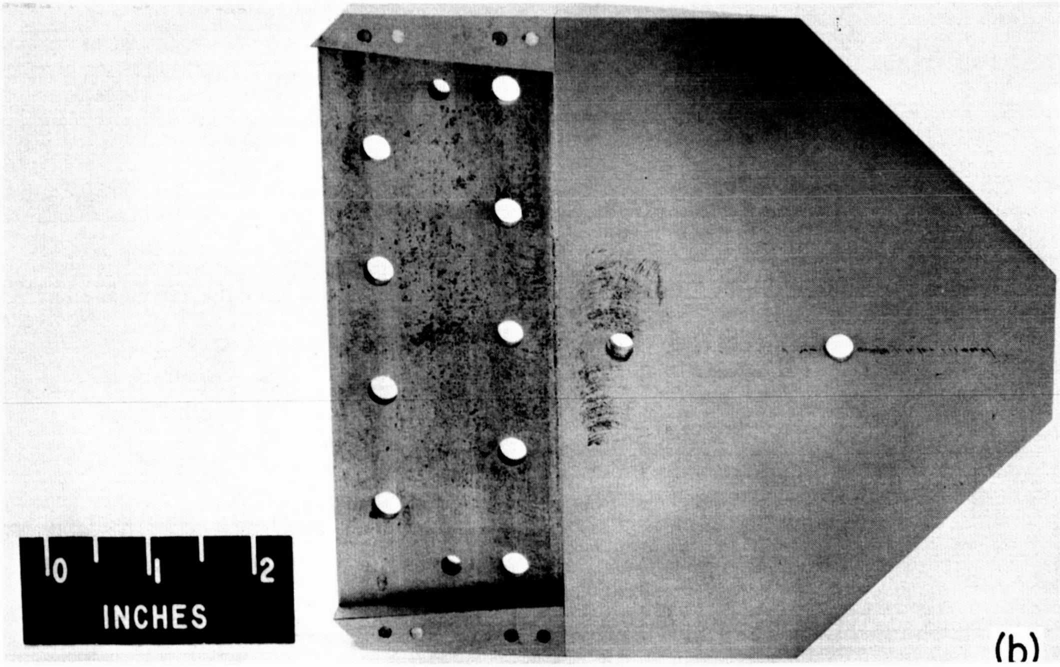

(b) Splitter plate 2.

Figure 5.- Splitter plates.

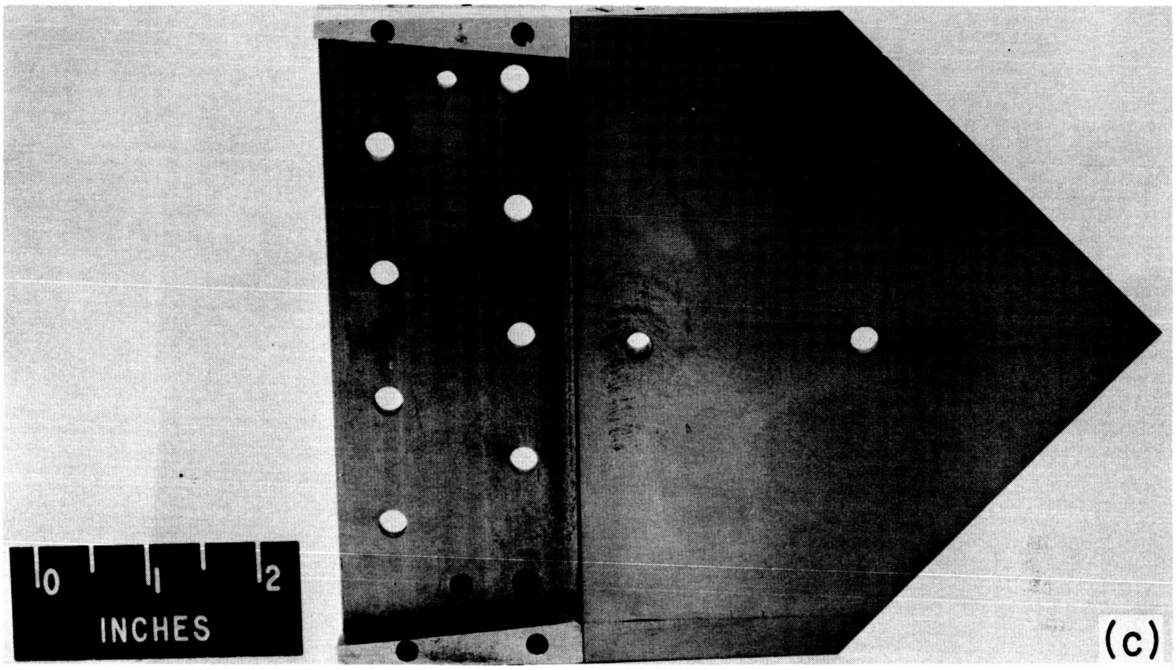

(c) Splitter plate 3.

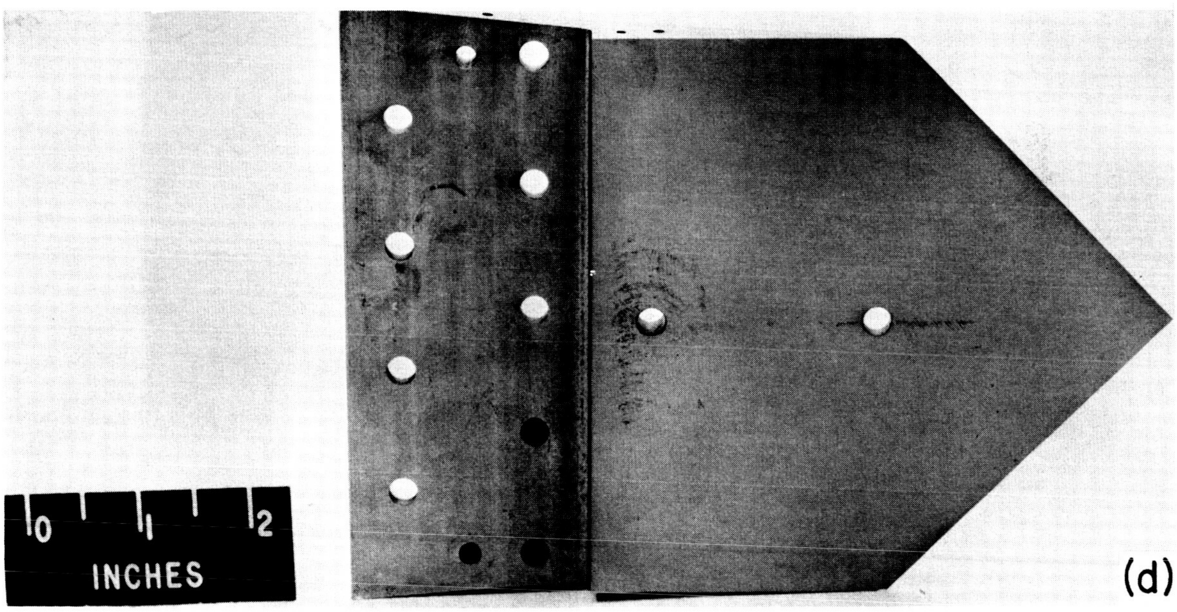

(d) Splitter plate 4.

Figure 5.- Continued.

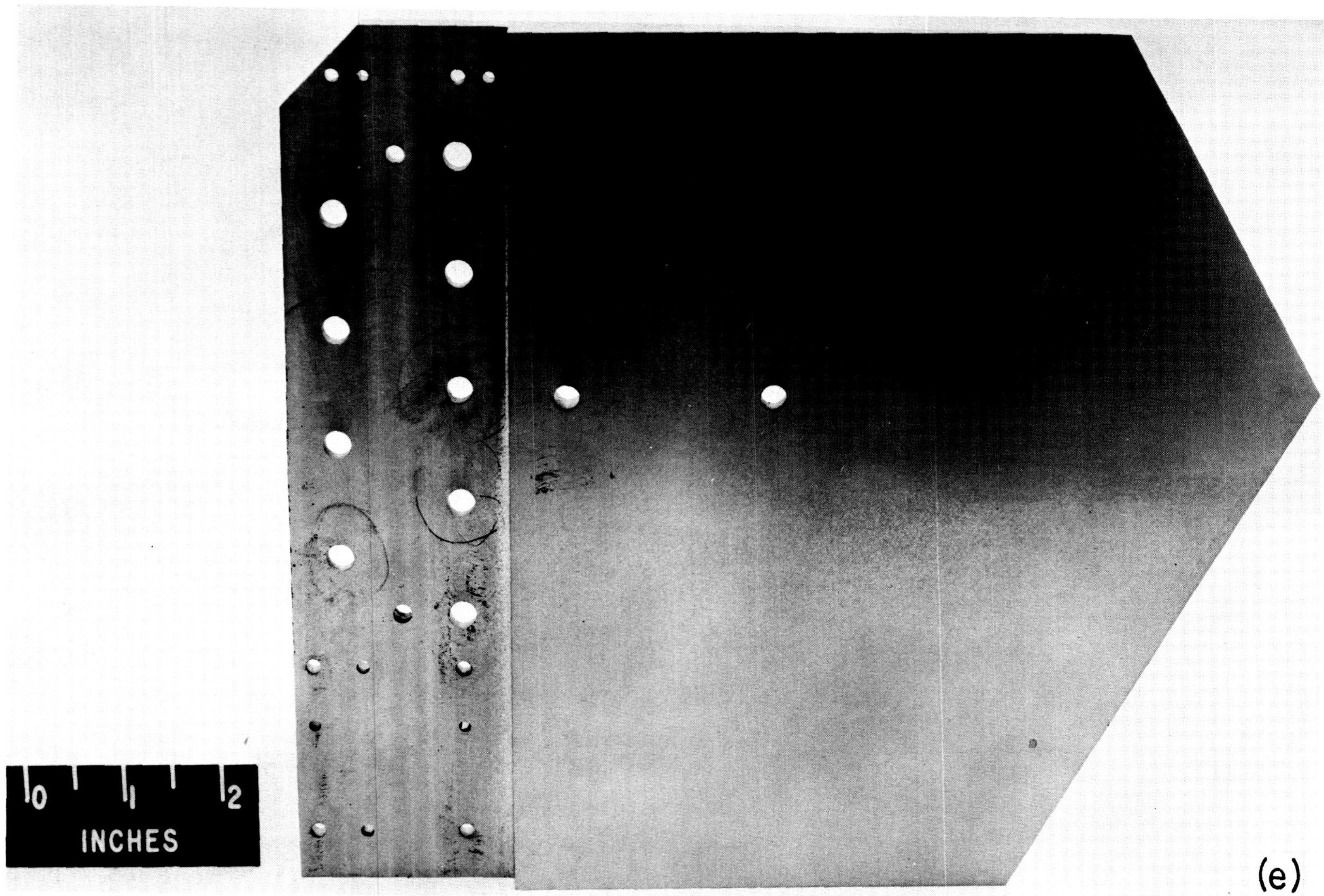

(e) Splitter plate 5.

Figure 5.- Concluded.

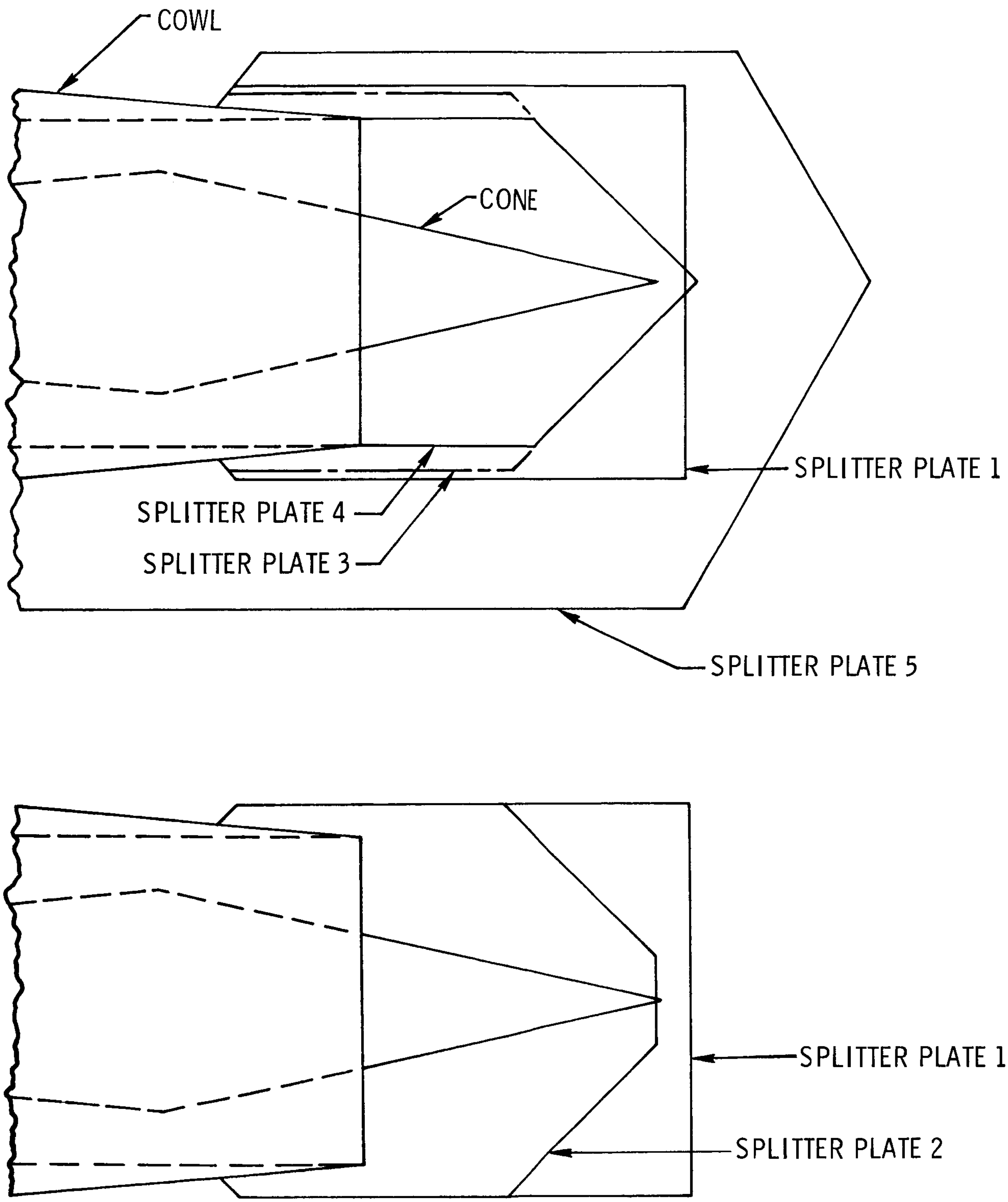

Figure 6.- Composite drawings of mounted splitter plates.

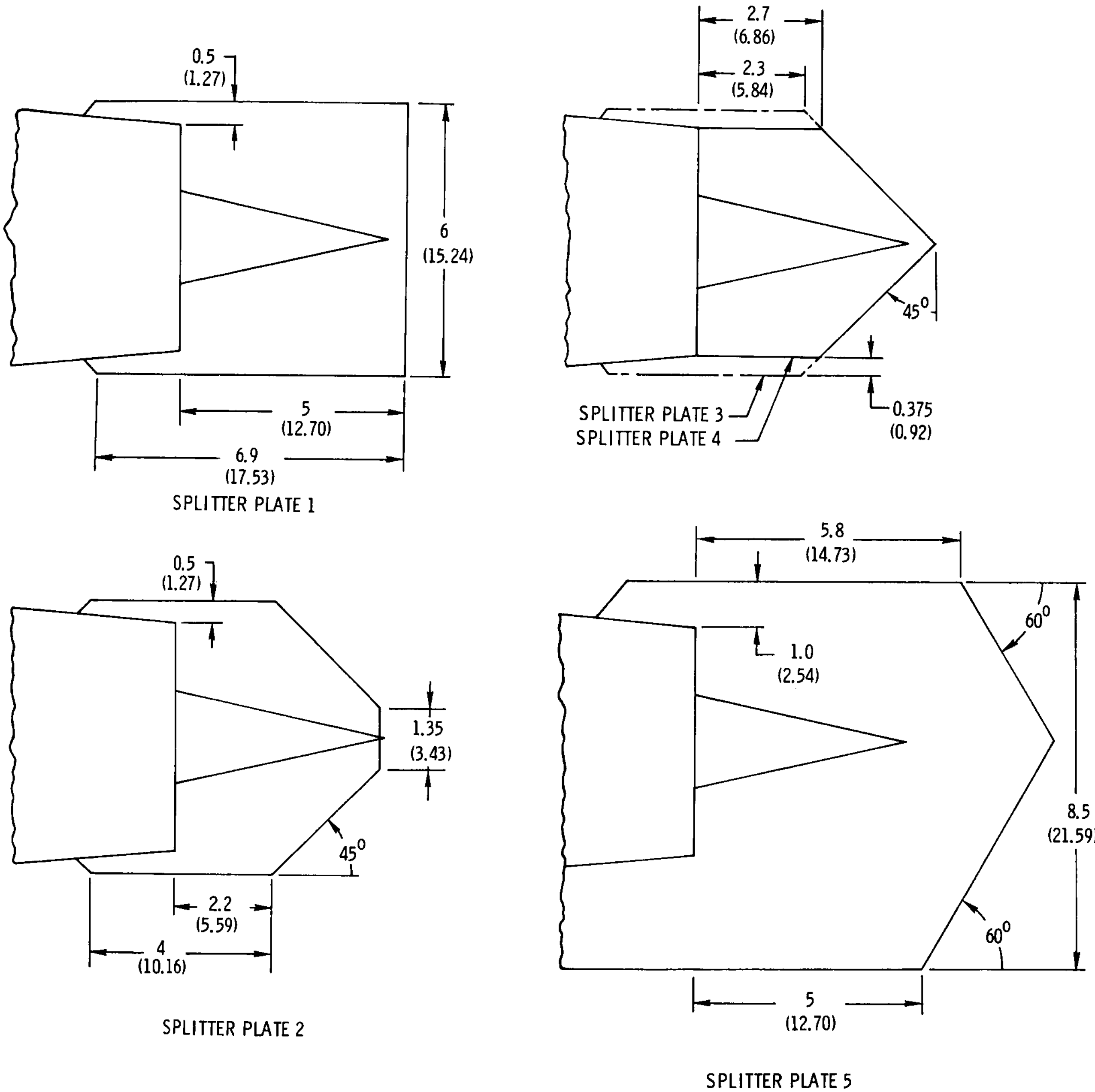

Figure 7.- Dimensional drawings of mounted splitter plates. All dimensions in inches (dimensions in parenthesis in centimeters).

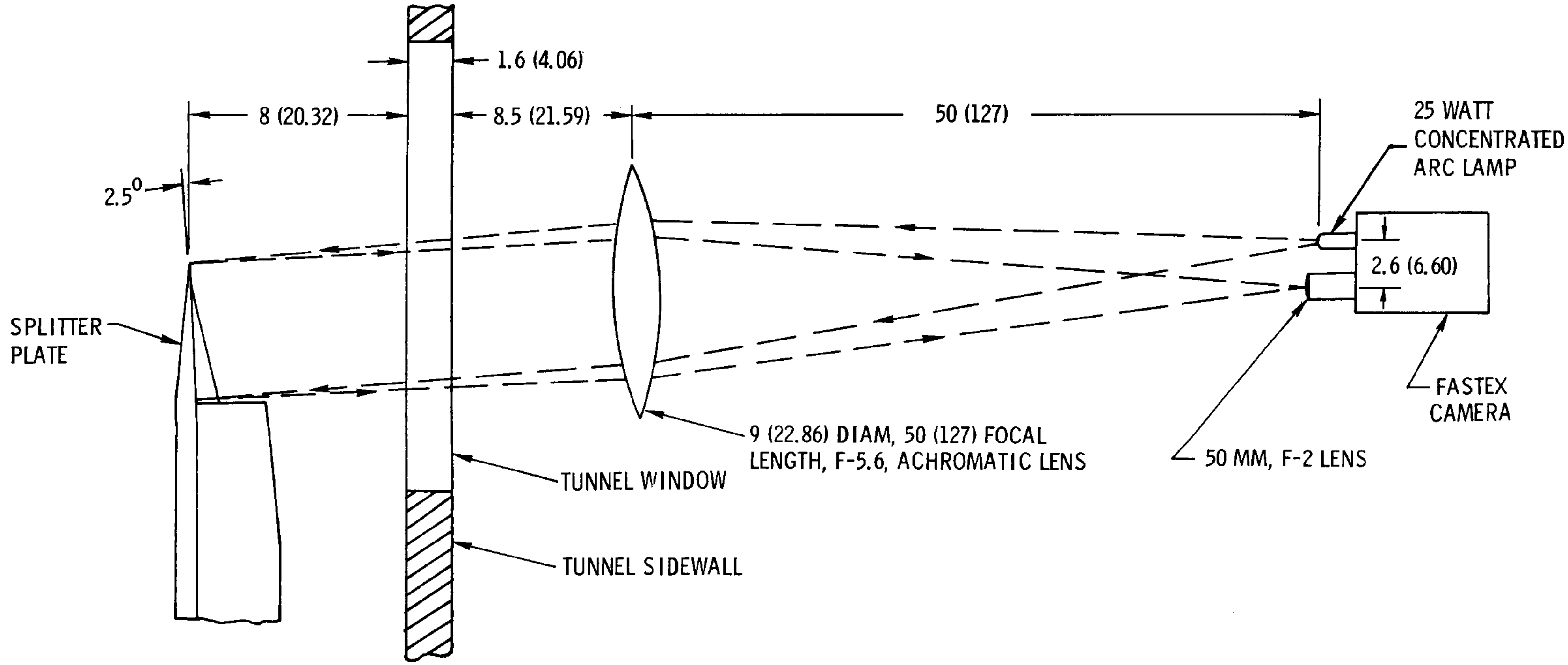

Figure 8.- Schematic drawing of shadowgraph system. All dimensions in inches (dimensions in parenthesis in centimeters).

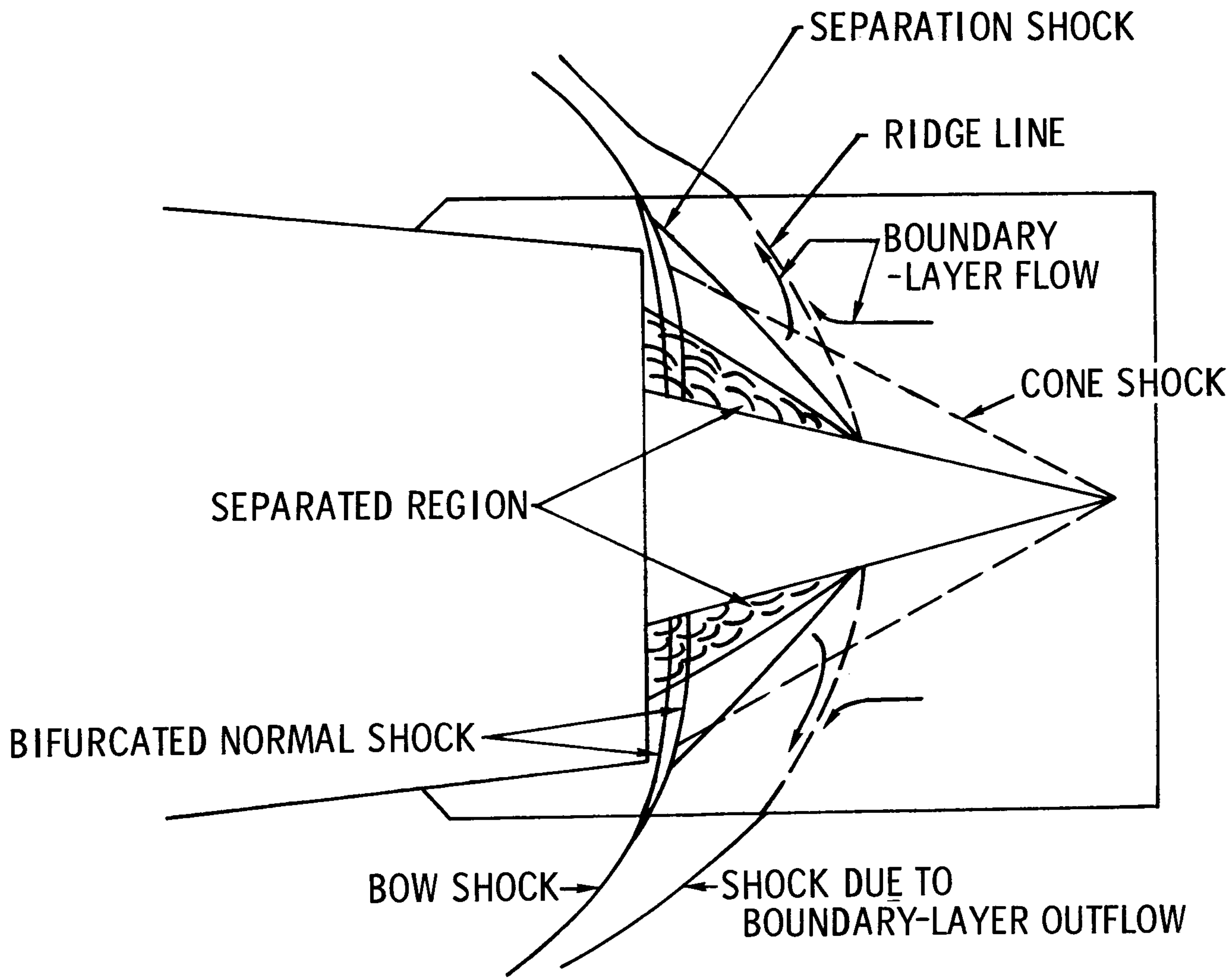

Figure 9.- Sketch of typical inlet-flow field.

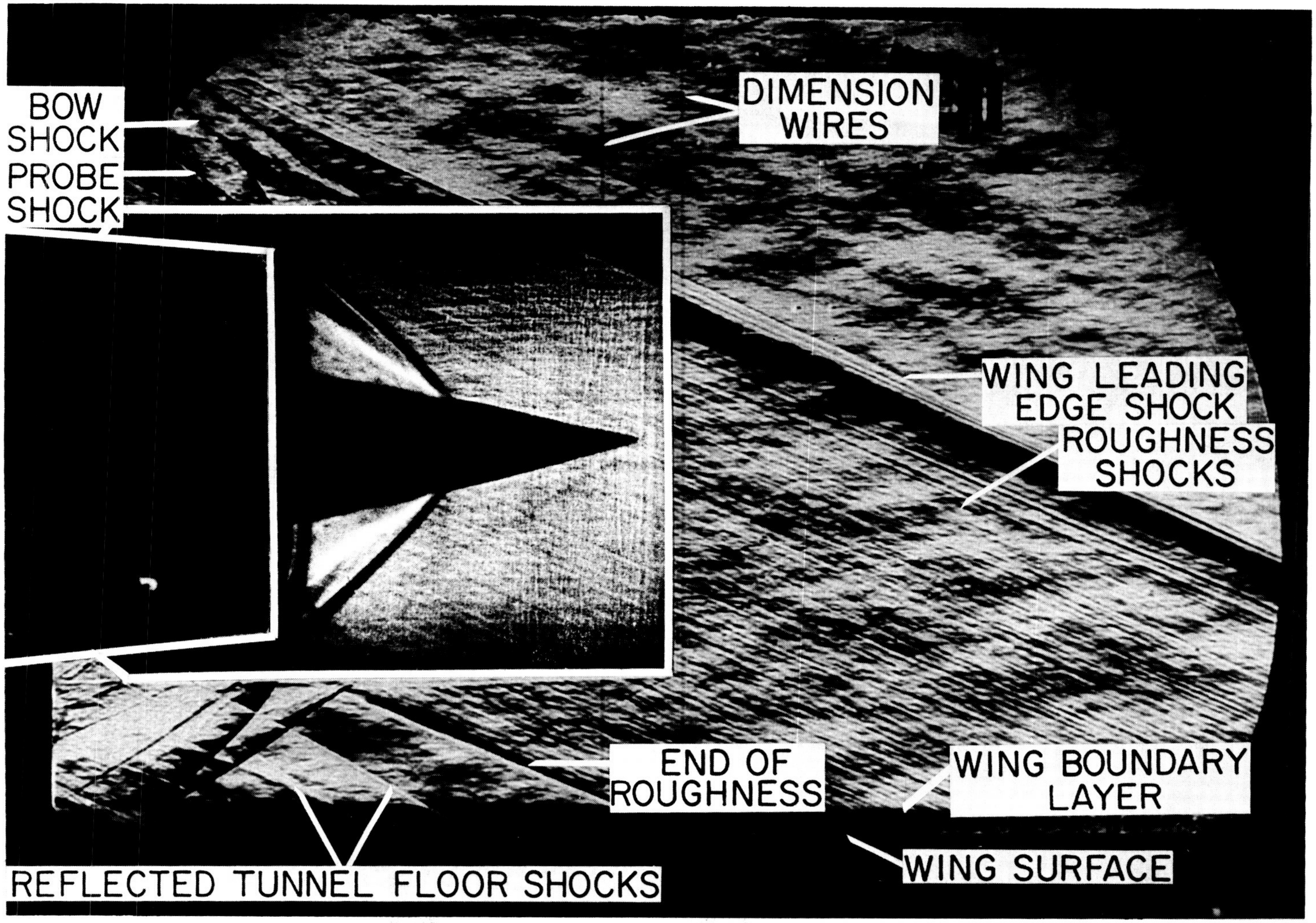

Figure 10.- Composite shadowgraph and schlieren of the flow, splitter plate 1, high pylon, $\psi = 0^{\circ}$, $\dot{m}_2/\dot{m}_1 = 0.72$.

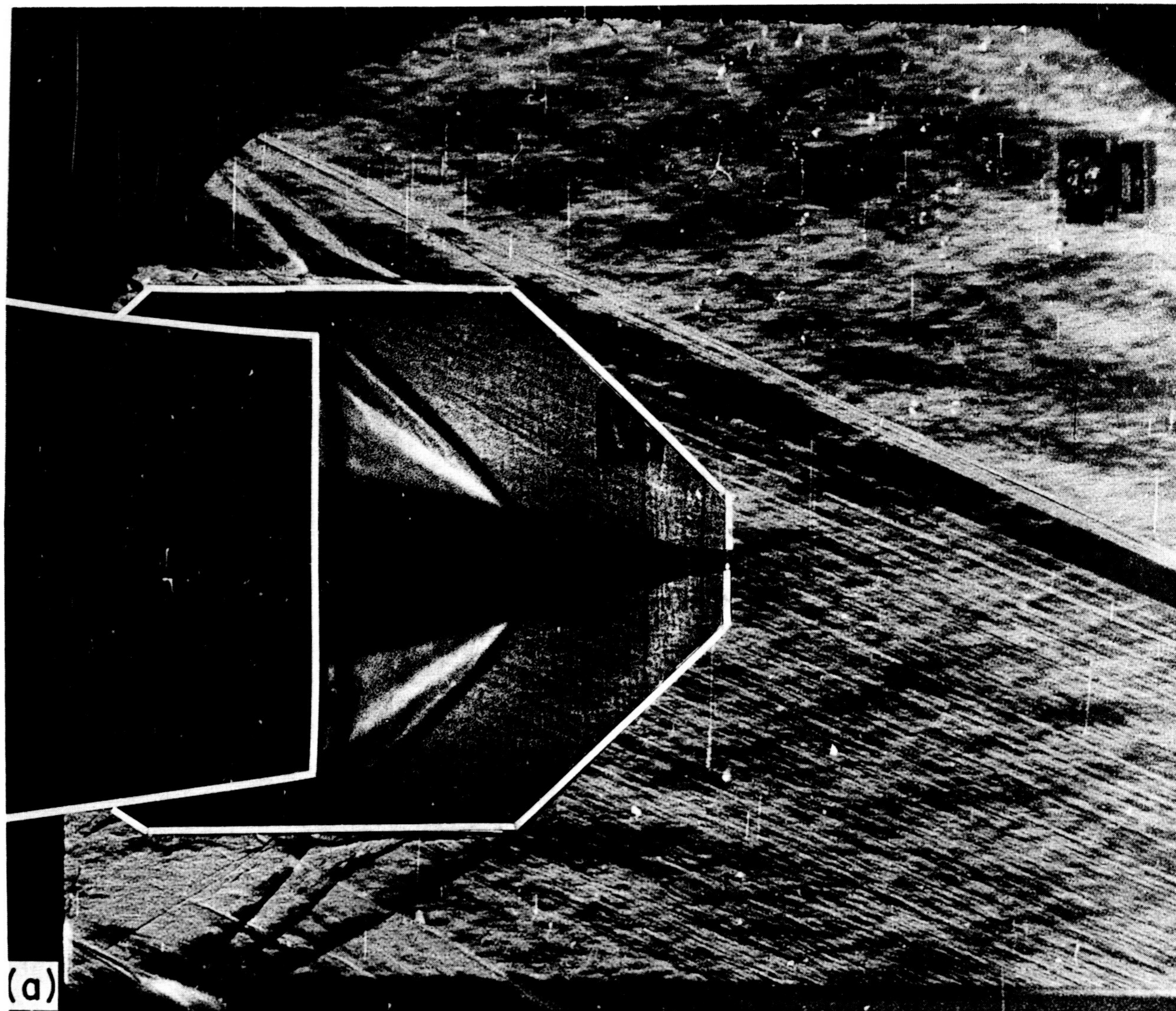

(a) Splitter plate 2.

Figure 11.- Composite shadowgraph and schlieren of the flow, high pylon, $\psi = 0^{\circ}$, $\dot{m}_2/\dot{m}_1 = 0.72$.

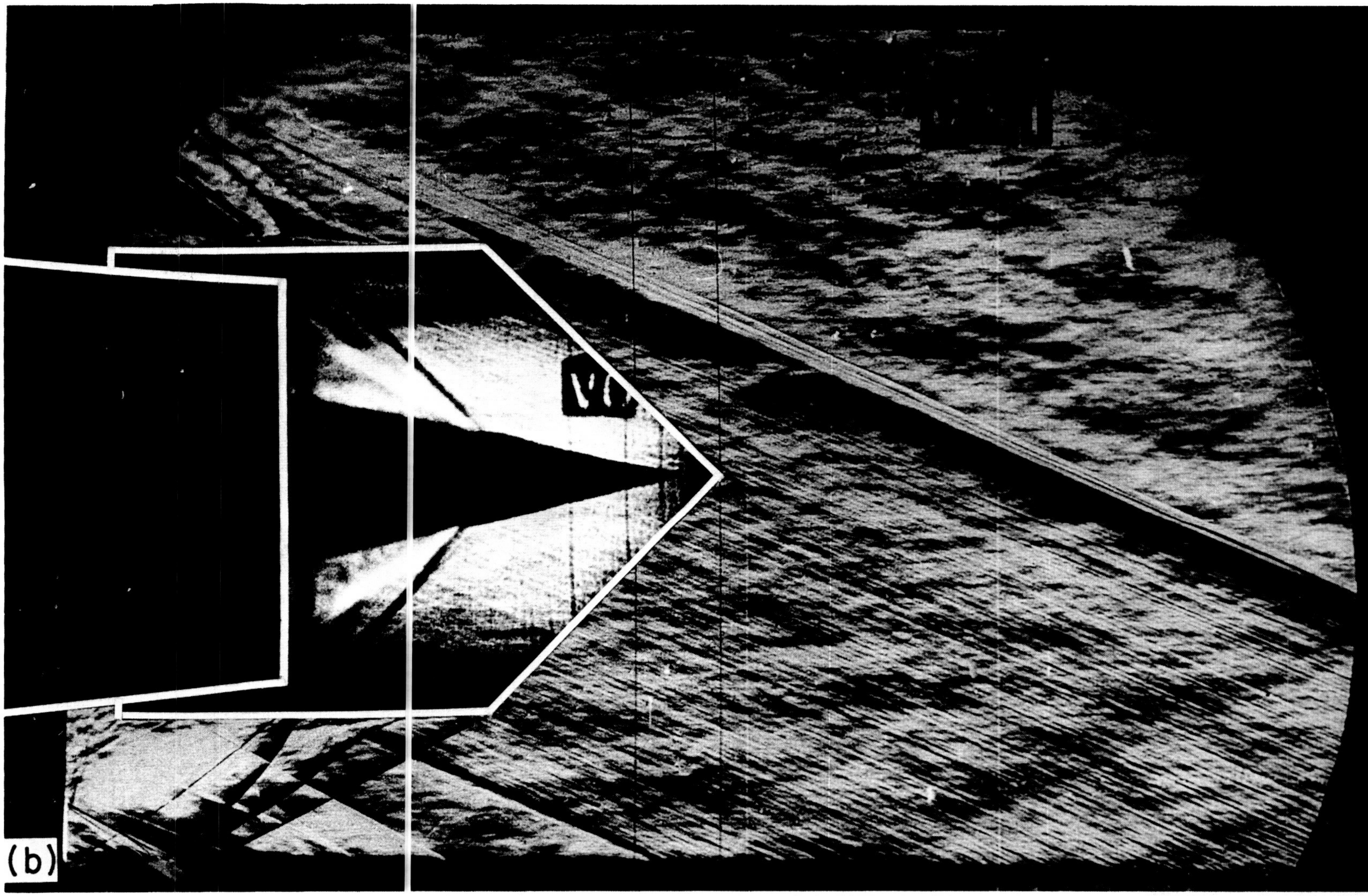

(b) Splitter plate 3.

Figure 11.- Continued.

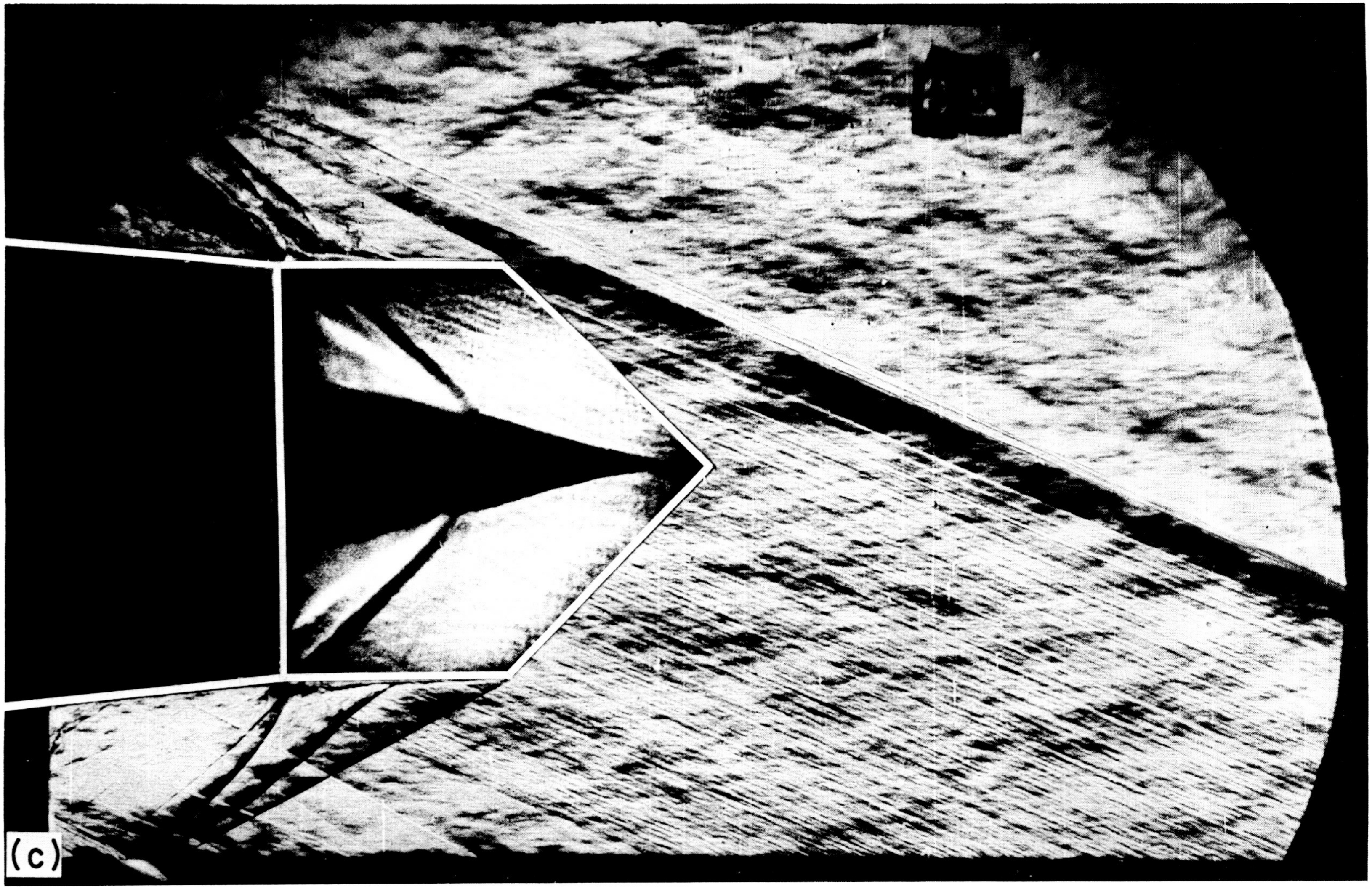

(c) Splitter plate 4.

Figure 11.- Concluded.

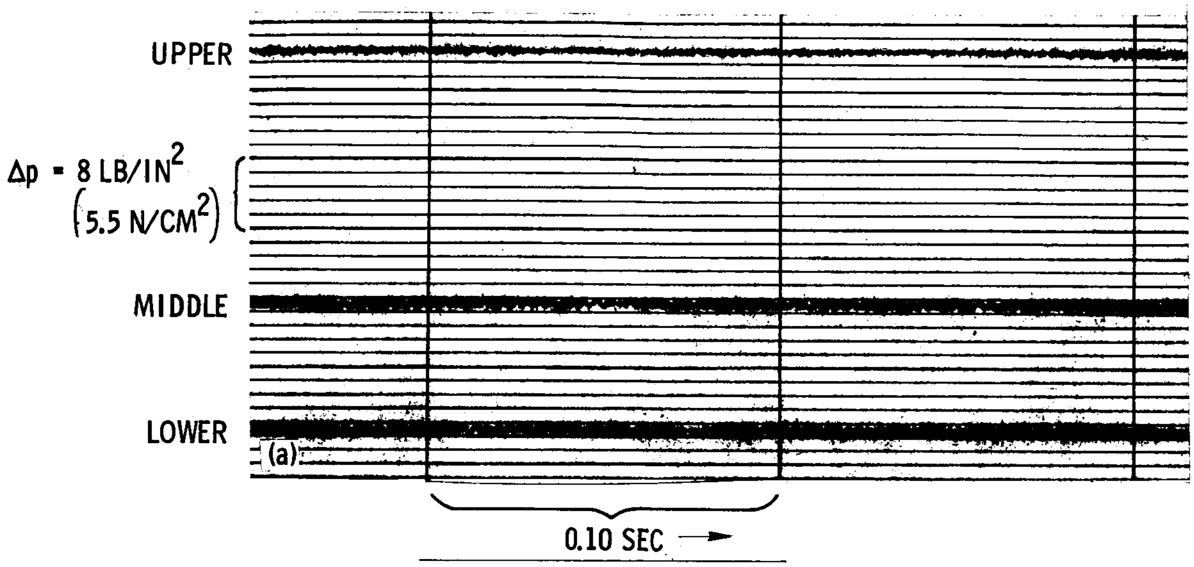

(a) Splitter plate 1.

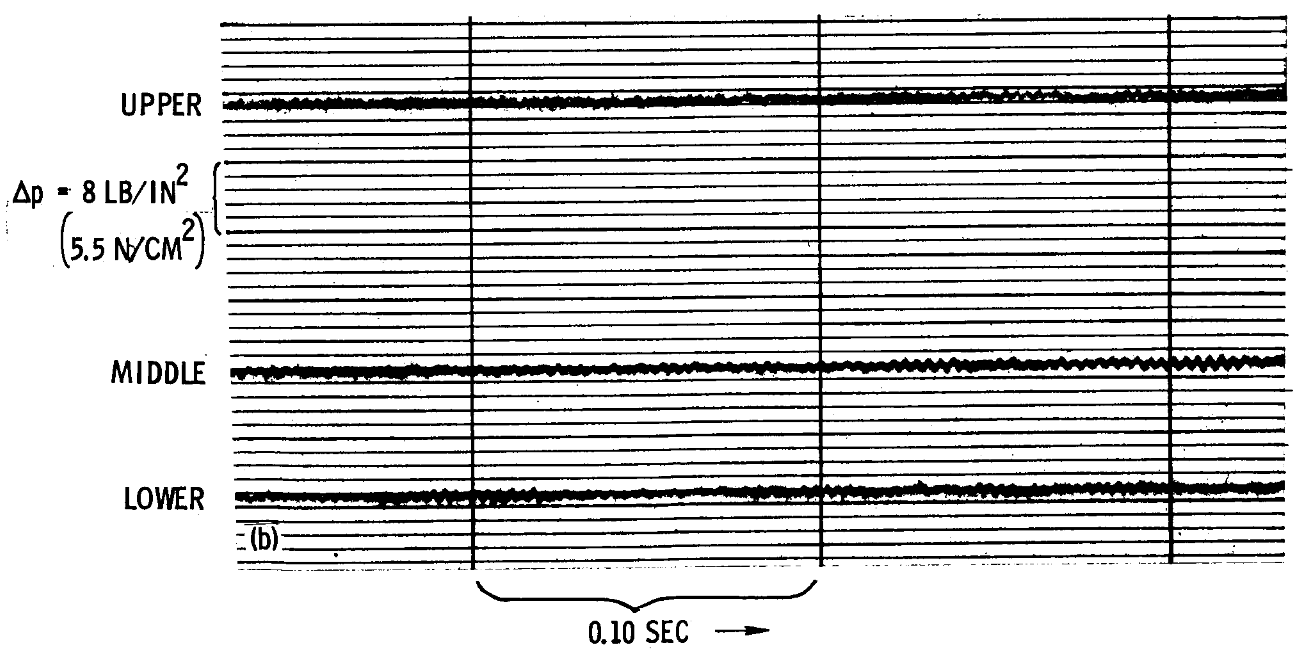

(b) Splitter plate 2.

Figure 12.- Pressure traces, high pylon, $\psi = 0^{\circ}$, $\dot{m}_2/\dot{m}_1 = 0.72$.

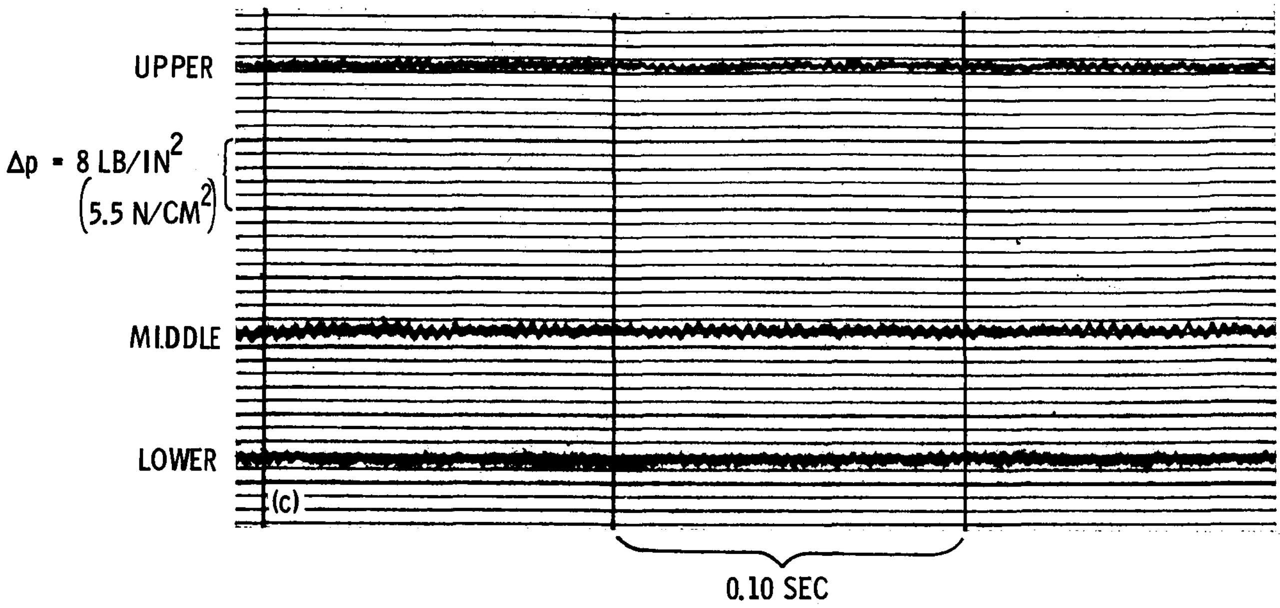

(c) Splitter plate 3.

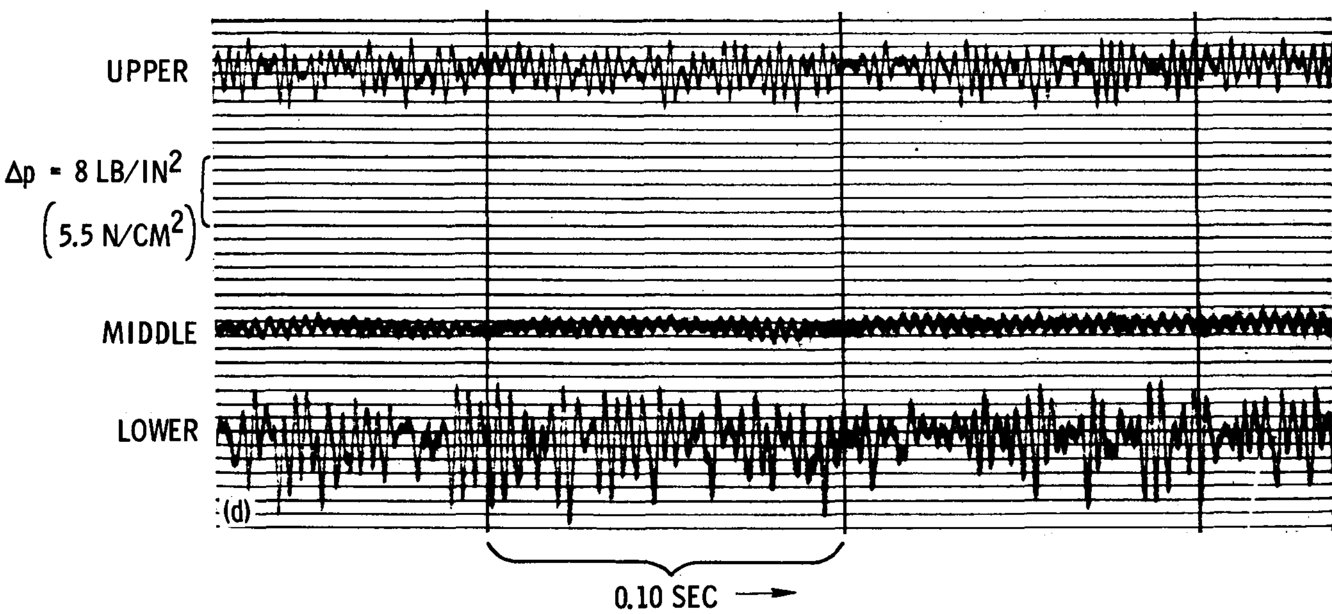

(d) Splitter plate 4.

Figure 12.- Concluded.

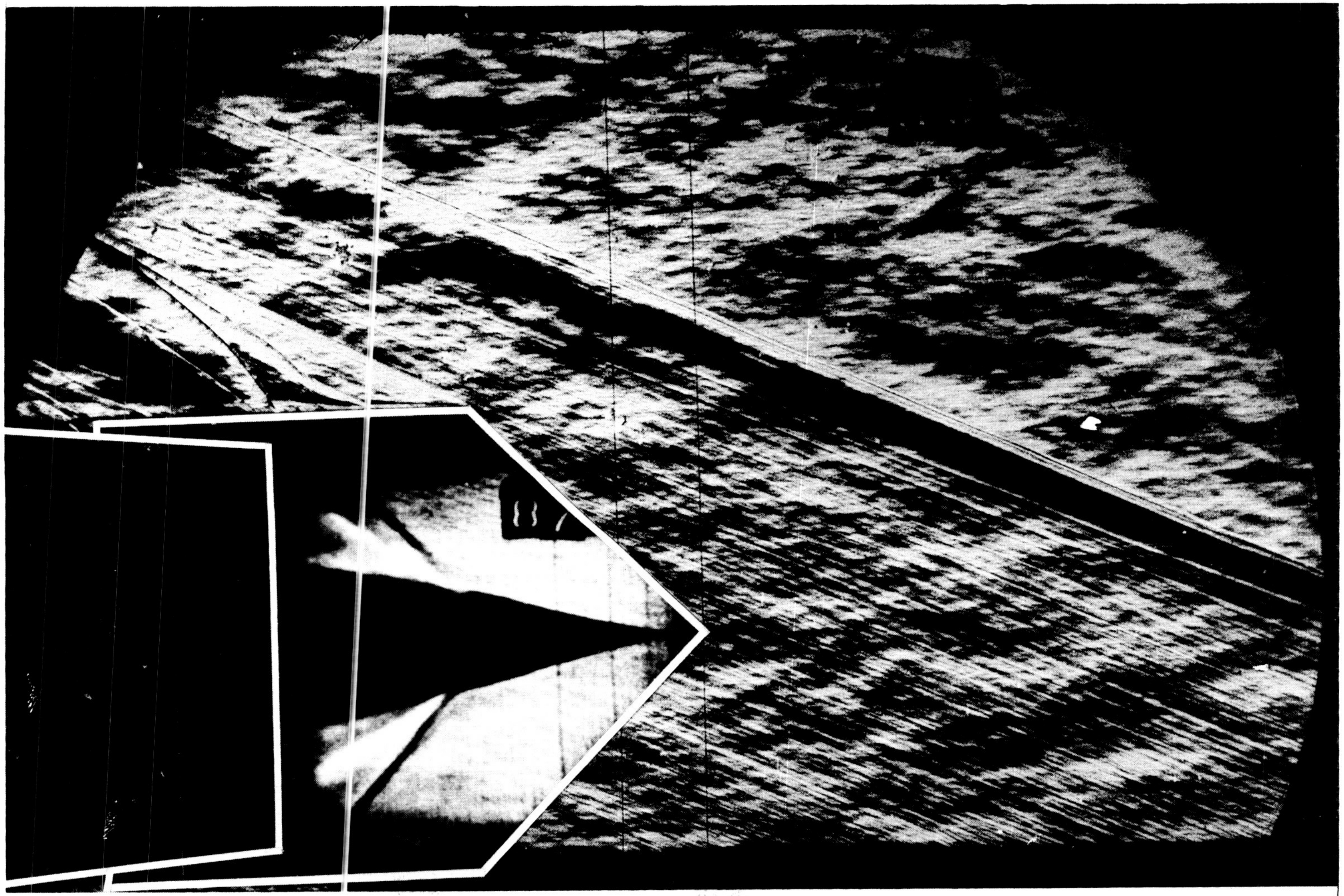

Figure 13.- Composite shadowgraph and schlieren of the flow, splitter plate 3, low pylon, $\psi = 0^{\circ}$, $\dot{m}_2/\dot{m}_1 = 0.71$.

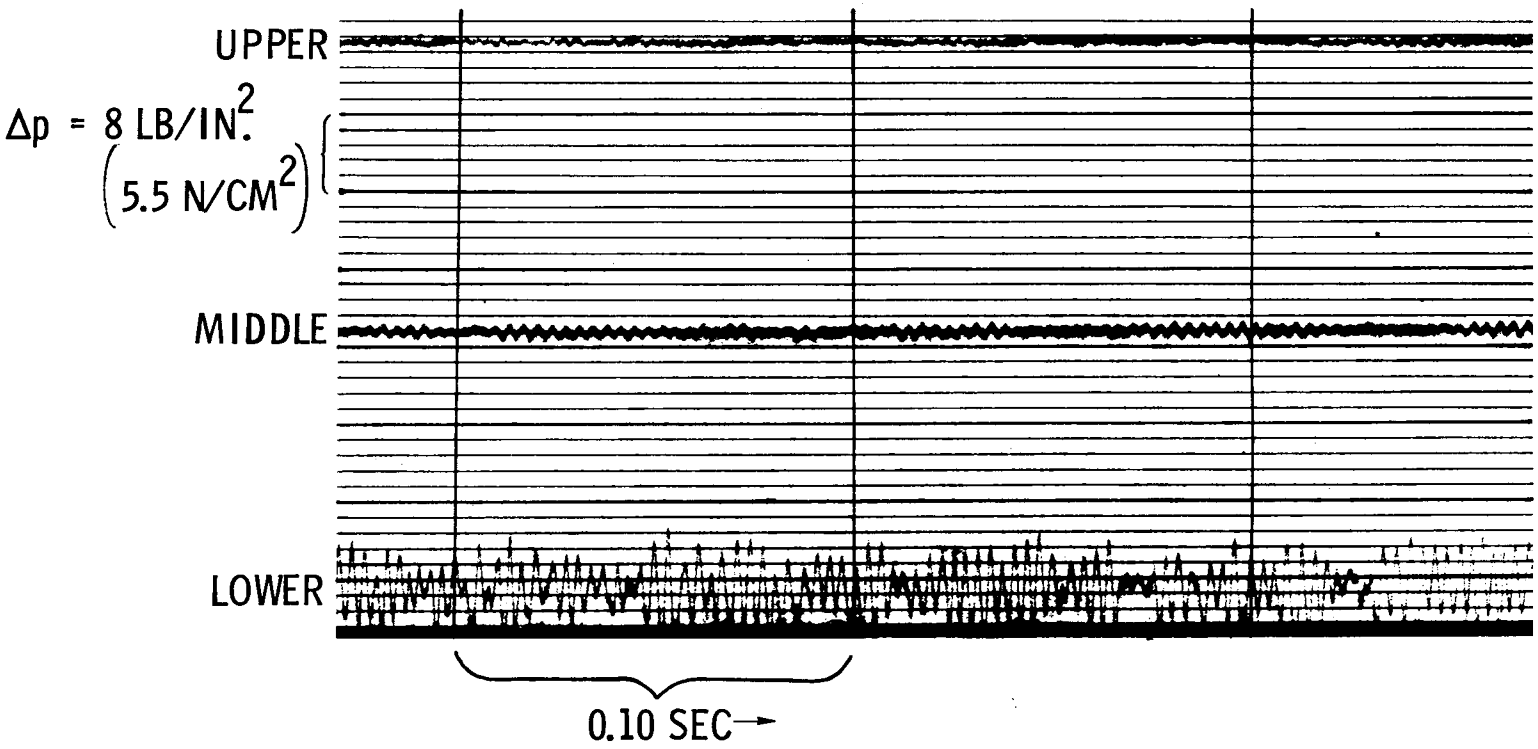

Figure 14.- Pressure traces, splitter plate 3, low pylon, $\psi = 0^{\circ}$, $\dot{m}_2/\dot{m}_1 = 0.71$.

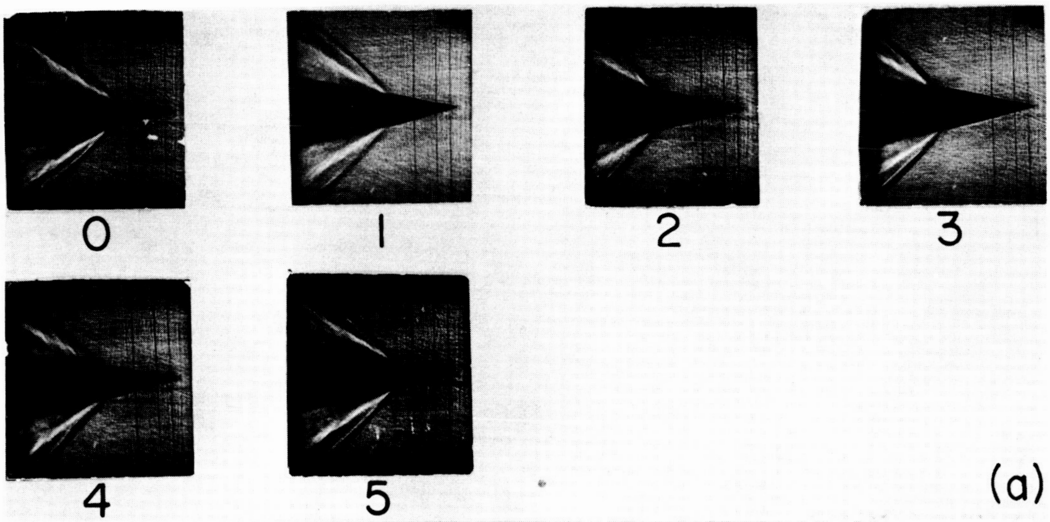

(a) $\dot{m}_2/\dot{m}_1 = 0.65$.

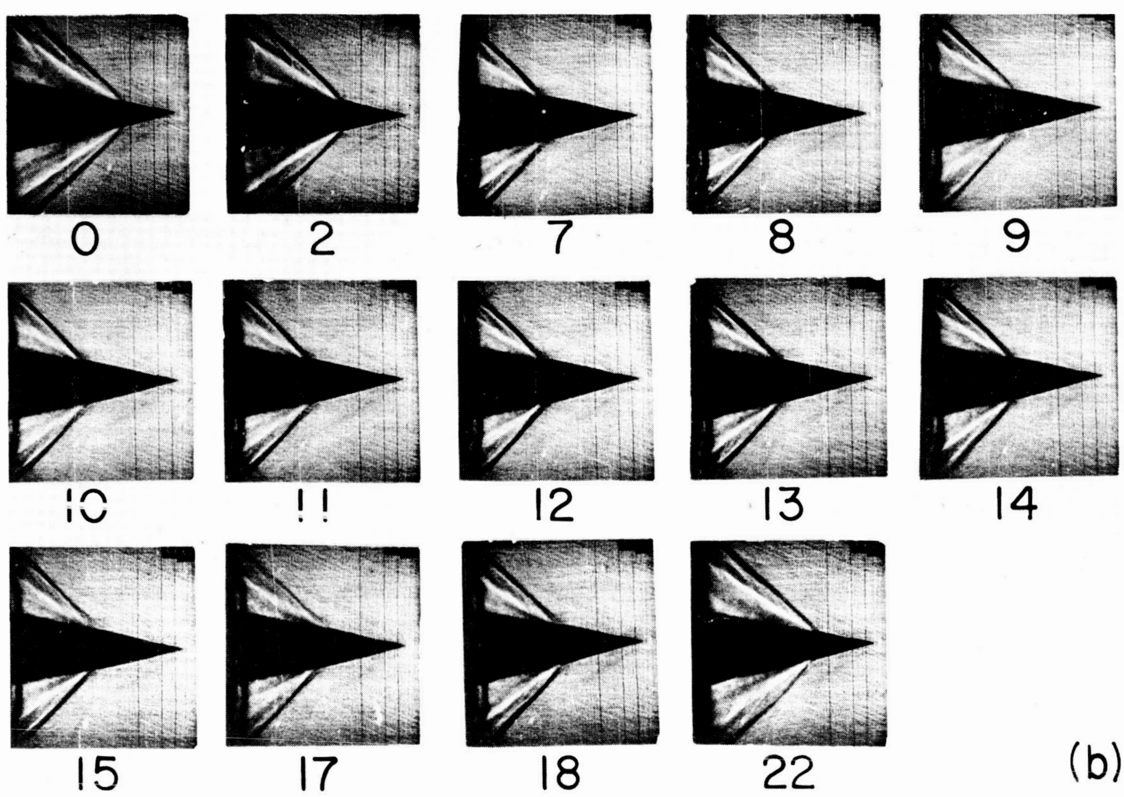

(b) $\dot{m}_2/\dot{m}_1 = 0.63$.

Figure 15.- Shadowgraphs of the flow, 2000 frames/sec, splitter plate 1, $\psi = 0^{\circ}$, high or medium pylon.

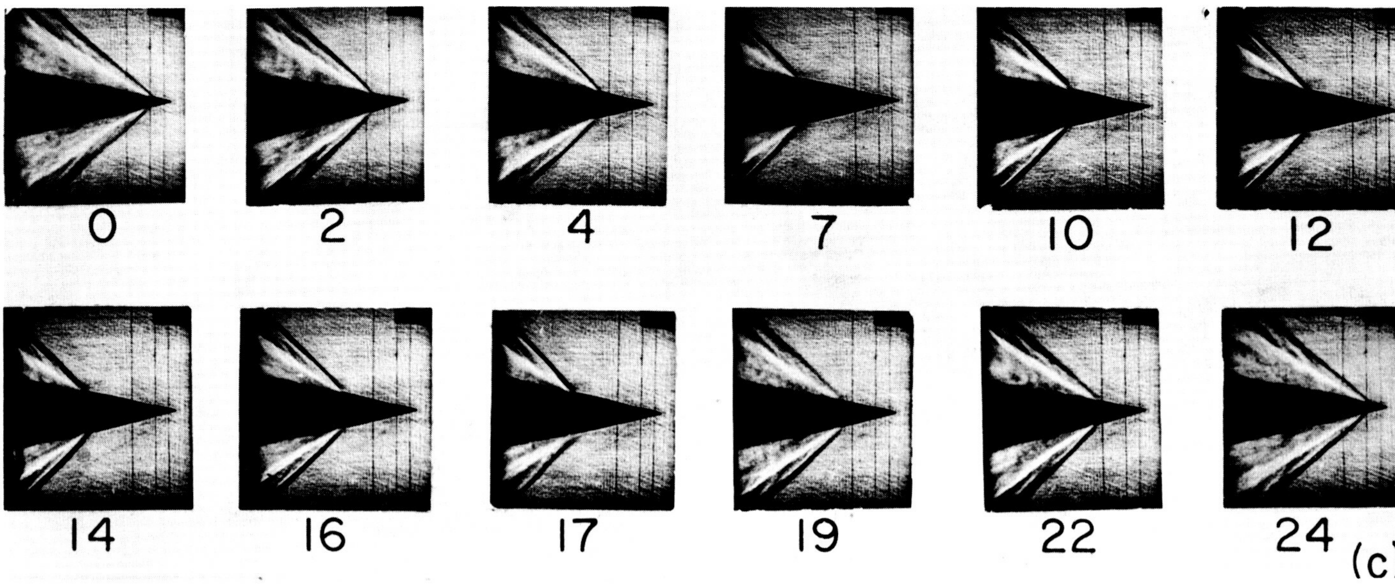

(c) $\dot{m}_2/\dot{m}_1 = 0.57$.

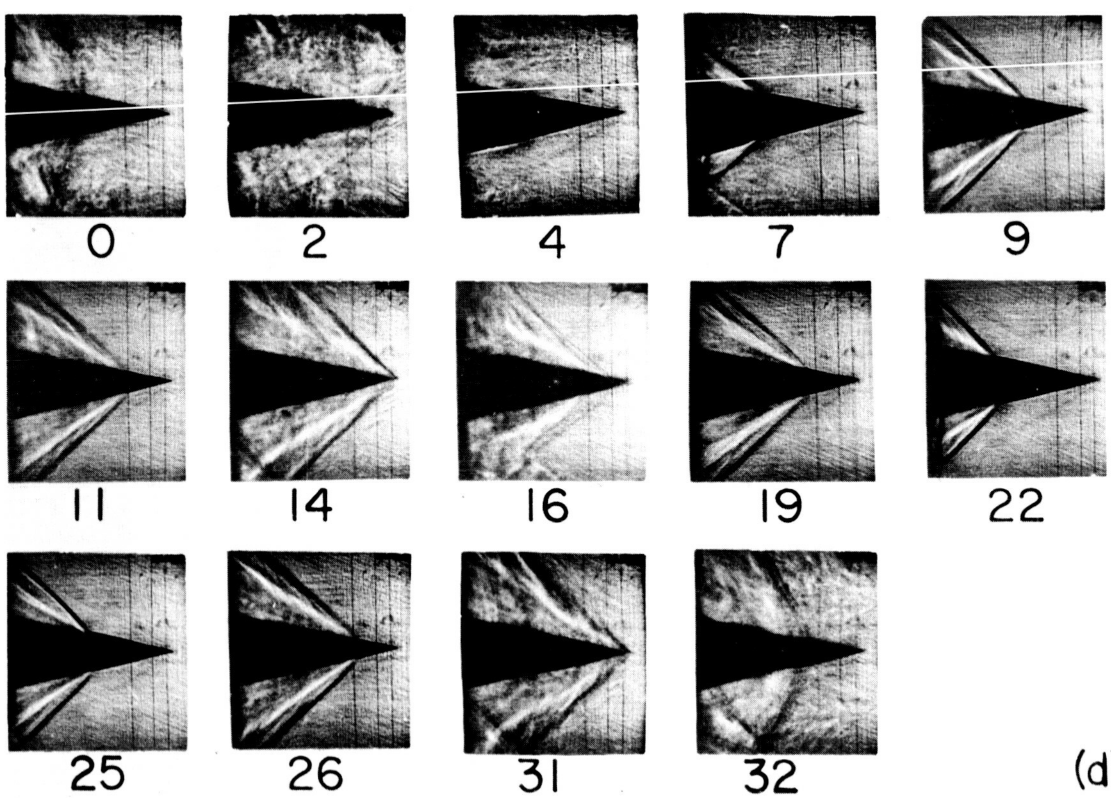

(d) $\dot{m}_2/\dot{m}_1 = 0.44$.

Figure 15.- Concluded.

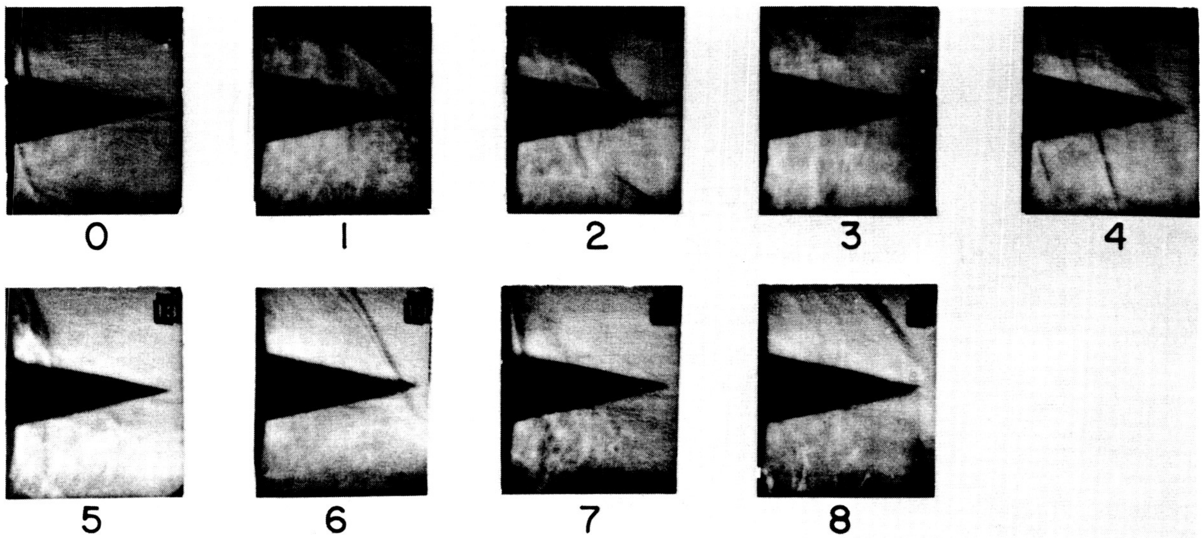

Figure 16.- Shadowgraphs of the flow, 750 frames/sec, splitter plate 1, high pylon, $\psi = 0^{\circ}$, $\dot{m}_2/\dot{m}_1 = 0$.

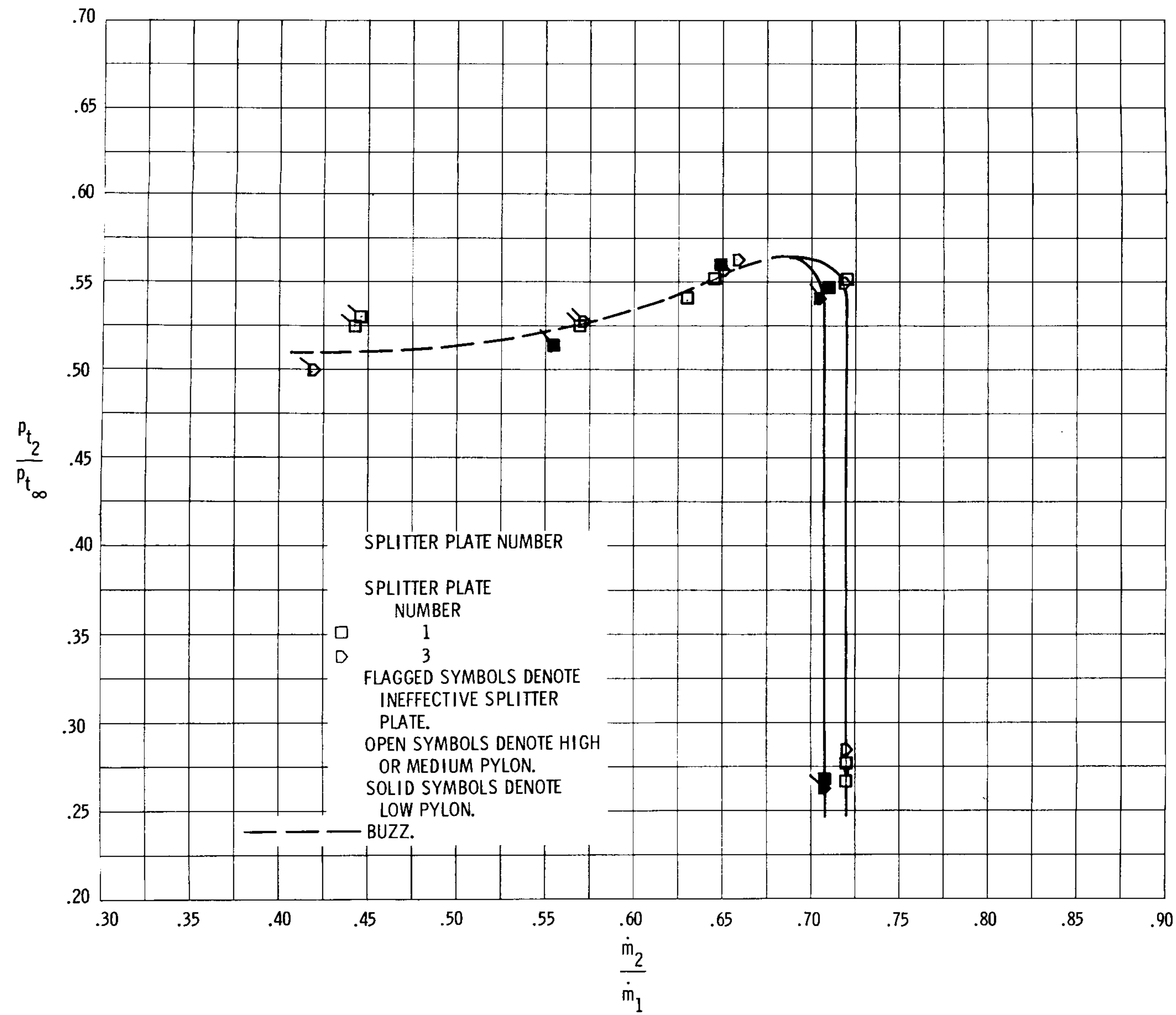

(a) Splitter plates 1 and 3.

Figure 17.- Pressure recovery versus mass-flow ratio, $\psi = 0^{\circ}$.

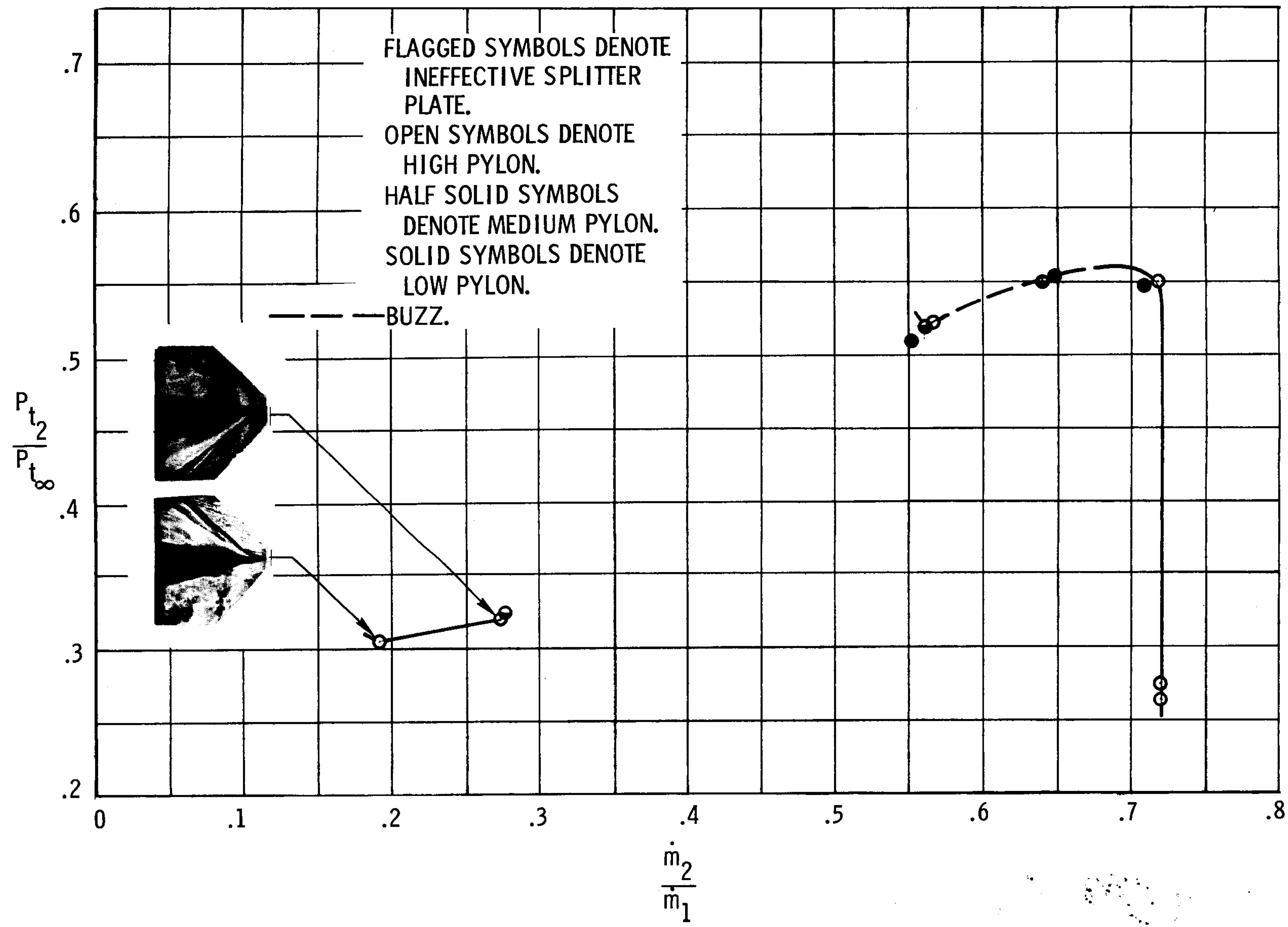

(b) Splitter plate 2.

Figure 17.- Concluded.

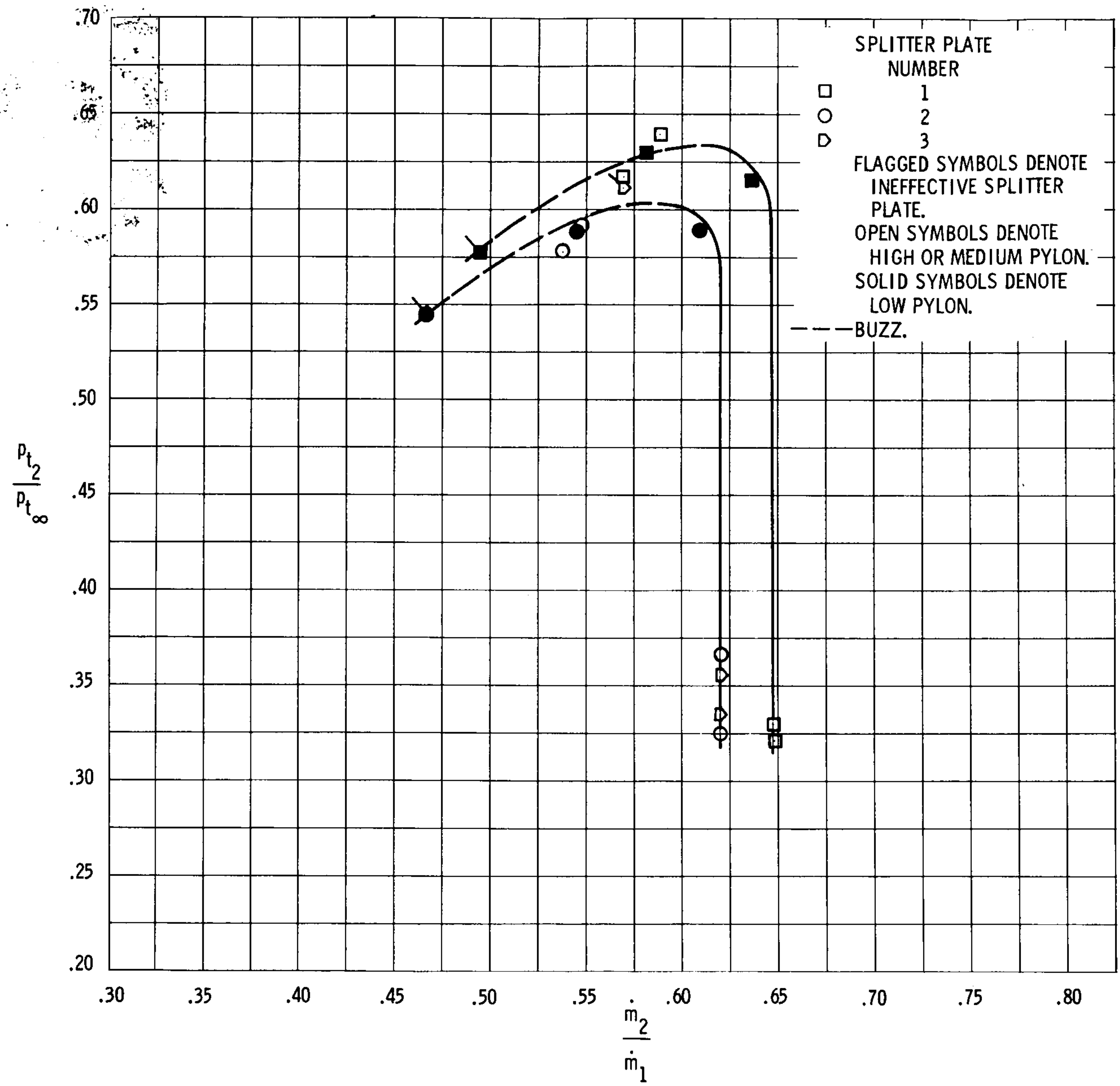

Figure 18.- Pressure recovery versus mass-flow ratio, $\psi = 6^{\circ}$.

NASA-Langley, 1965